spinal motoneurons in mutant SOD1-tg animals as well as in patients with familial and sporadic ALS (Estévez et al., 1998; Cleveland, 1999; Cleveland and Rothstein, 2001). If motoneuron degeneration after peripheral nerve avulsion shares any underlying mechanisms of motoneuron death associated with SOD1 mutation, motoneurons in presymptomatic mutant SOD1-tg animals may be more susceptible to pathological insults following avulsion compared with their non-tg littermates. If this is so, we may be able to utilize facial nerve avulsion as an animal model for understanding the mechanisms of motoneuron degeneration in ALS. In the present study, we examined injured motoneurons after facial nerve avulsion in presymptomatic mutant human SOD1-tg rats and their littermates.

MATERIALS AND METHODS

Animals and Surgical Procedures

The experimental protocols were approved by the Institutional Animal Care and Use Committee of Tokyo Metropolitan Institute for Neuroscience and Tohoku University Graduate School of Medicine. The tg rats expressing human mutant SOD1 (H46R, G93A) were generated as described previously (Nagai et al., 2001). Two types of rats with SOD1 mutations, H46R and G93A, were used for experiments. The H46R-tg rats develop motor deficits at about 140 days of age and die after 3 weeks, and G93A-tg rats show the clinical signs at around 120 days of age and die after 10 days (Nagai et al., 2001).

The presymptomatic female H46R (90 days old)- and G93A (80 days old)-tg rats were anesthetized with inhalation of halothane. Under a dissecting microscope, the right facial nerve was exposed at its exit from the stylomastoid foramen. With microhemostat forceps, the proximal facial nerve was avulsed by gentle traction and removed from the distal facial nerve as described elsewhere (Sakamoto et al., 2000, 2003a,b; Ikeda et al., 2003). As for axotomy, the right facial nerve was transected at its exit from the stylomastoid foramen, and a distal portion of the nerve, 5 mm in length, was cut and removed. The wound was covered with a small piece of gelatin sponge (Gelfoam; Pharmacia Upjohn, Bridgewater, NJ) and closed by fine suture.

Motoneuron Cell Counting

At 2 weeks postoperation, rats were anesthetized with a lethal dose of pentobarbital sodium and transcardially perfused with 0.1 M phosphate buffer, pH 7.4 (PB), followed by 4% paraformaldehyde in 0.1 M PB. The brainstem tissue was excised, postfixed in the same fixative for 2 hr, dehydrated, and embedded in paraffin, and serial transverse sections (6-μm thickness) were made. Every fifth section (24-μm interval) was collected, deparaffinized, and stained with cresyl violet (Nissl staining), and facial motoneurons having nuclei containing distinct nucleoli on both sides of the facial nuclei were counted in 25 sections as described elsewhere (Sakamoto et al., 2000, 2003a,b; Ikeda et al., 2003). The data were expressed as the mean ± SEM, and statistical significance was assessed by Mann-Whitney U-test.

Immunohistochemistry

Immunohistochemistry on paraffin sections was performed with the following primary antibodies: sheep anti-human SOD1 (1:1,000; Calbiochem, San Diego, CA), rabbit anti-human SOD1 (1:10,000; kindly provided by Dr. K. Asayama; Asayama and Burr, 1984), mouse monoclonal anti-phosphorylated neurofilament SMI-31 (1:1,000; Sternberger Monoclonals, Lutherville, MD), rabbit anti-ubiquitin (1:1,000; Dako, Glostrup, Denmark), rabbit anti-glial fibrillary acidic protein (GFAP; 1:1,000; Dako), rabbit anti-activating transcription factor-3 (ATF3; sc-188, 1:200; Santa Cruz Biotechnology, Santa Cruz, CA), rabbit anti-c-Jun (sc-1694, 1:200; Santa Cruz Biotechnology), mouse monoclonal anti-phosphorylated c-Jun (sc-822, 1:200; Santa Cruz Biotechnology), rabbit anti-heat shock protein (Hsp) 25 that reacts with rat Hsp27 (SPA-801, 1:200; Stressgen, Victoria, British Columbia, Canada), and rabbit anti-phosphospecific (Ser^{15})Hsp27 (1:200; Oncogene, San Diego, CA). For immunohistochemistry, deparaffinized sections were pretreated with 0.3% H_2O_2 in methanol and preincubated with 3% heat-inactivated goat or rabbit serum in 0.1% Triton X-100 in phosphate-buffered saline (T-PBS). In cases of immunostaining with mouse primary antibodies, MOM blocking kit (Vector, Burlingame, CA) was used according to the manufacturer's instructions to reduce nonspecific background staining. Sections were then incubated overnight at 4°C with the primary antibodies diluted in T-PBS, followed by the incubation with biotinylated rabbit anti-sheep, goat anti-rabbit, or goat anti-mouse IgG at a dilution of 1:200 and with ABC reagent (Vector), visualized by 3,3′-diaminobenzidine tetrahydrocholoride (DAB)-H_2O_2 solution and counterstained with hematoxylin. For negative controls, the primary antibodies were omitted or replaced by nonimmunized animal sera.

RESULTS

Two weeks after avulsion of the right facial nerves in non-tg littermates, the number of surviving facial motoneurons declined to ~70% of that on the contralateral side, similar to that in normal rats, as described previously (Sakamoto et al., 2000). In SOD1-tg rats, only ~30–50% of motoneurons survived 2 weeks after avulsion, indicating that the loss of motoneurons was exacerbated in SOD1-tg rats compared with their non-tg littermates (Fig. 1, Table I). The numbers of surviving motoneurons in G93A-tg rats after avulsion (~35% of contralateral side) were significantly less than those in H46R-tg rats (~50% of contralateral side; Table I). The numbers of intact motoneurons at contralateral sides did not differ between tg rats and non-tg littermates, indicating that cell loss does not happen at this moment in the course of the disease with SOD1 mutations (Table I). Facial nerve axotomy did not induce significant loss of injured motoneurons in tg rats and non-tg littermates at 2 weeks postoperation (Fig. 1, Table I).

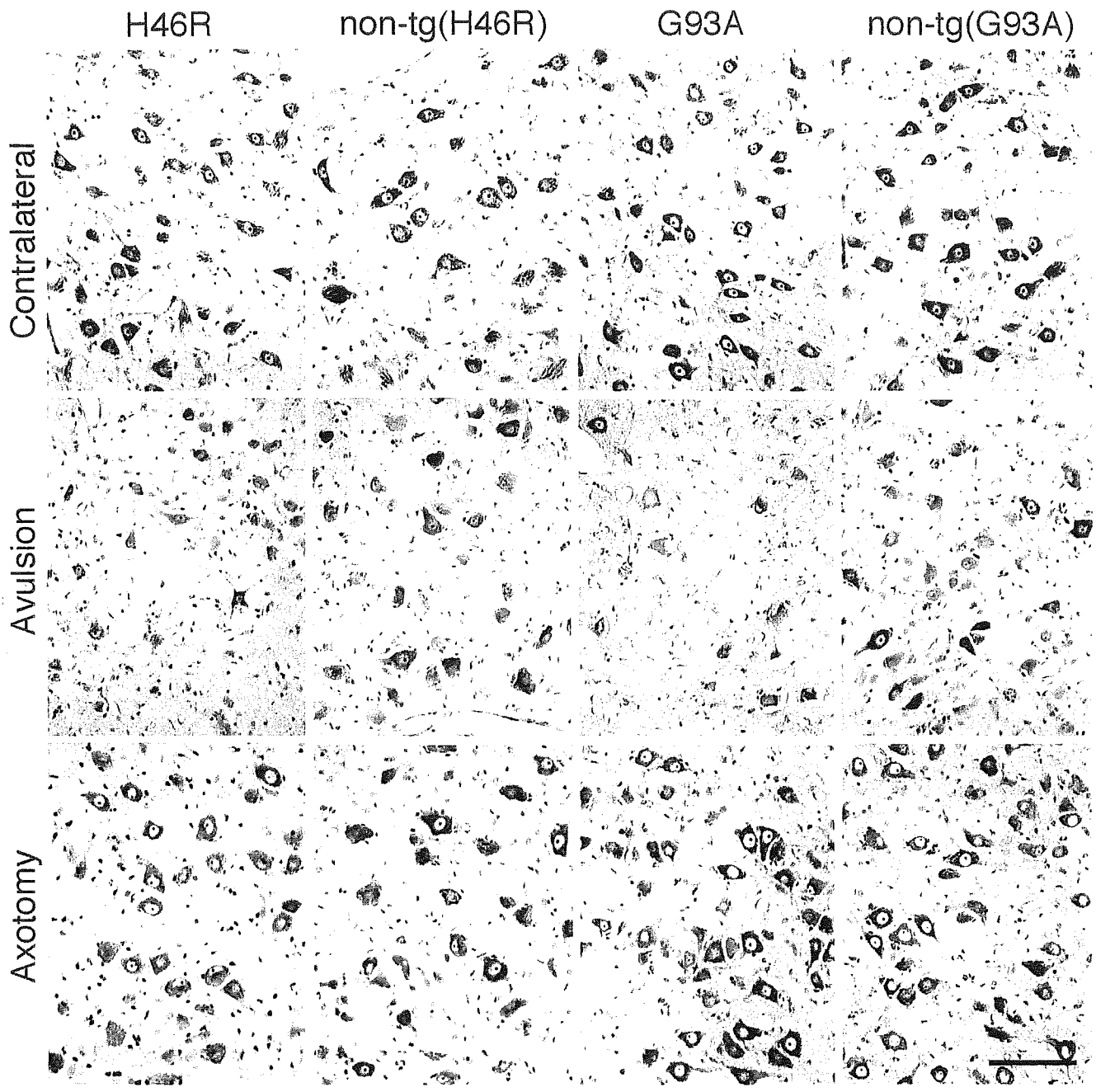

Fig. 1. Facial motoneurons of H46R- and G93A-transgenic (tg) rats and their non-tg littermates on the contralateral and ipsilateral (avulsion or axotomy) sides 2 weeks after facial nerve avulsion or axotomy. Nissl stain. Scale bar = 100 μm.

Examination of sections immunostained for SOD1 showed intense cytoplasmic immunolabeling for SOD1 in injured motoneurons after avulsion in H46R- and G93A-tg rats compared with uninjured motoneurons on the contralateral side that were not or were very faintly immunoreactive for SOD1 (Fig. 2). We used sheep and rabbit anti-SOD1 antibodies, both of which gave identical results. The cytoplasmic SOD1 immunolabeling patterns of injured motoneurons appeared diffuse in H46R-tg rats, whereas they were granular in G93A-tg rats. In G93A-tg rats, there were axons and vacuolar changes in the neuropil consistently immunoreactive for SOD1 at both uninjured and injured sides of facial nuclei (Fig. 2). There was no definite immunolabeling for SOD1 in either injured or uninjured motoneurons and their axons in non-tg littermates (Fig. 2). Facial nerve axotomy did not increase immunoreactivity for SOD1 in injured motoneurons of tg rats and non-tg littermates at 2 weeks

TABLE I. Survival of Motoneurons After Facial Nerve Avulsion and Axotomy[†]

Rat (n)	Ipsilateral motoneuron number	Contralateral motoneuron number	Survival %
Avulsion			
NL (H46R) (n = 10)	598 ± 18	813 ± 26	73.7 ± 1.2
H46R (n = 8)	402 ± 36*	839 ± 27	47.5 ± 2.8*
NL (G93A) (n = 6)	637 ± 56	822 ± 47	76.7 ± 3.0
G93A (n = 7)	306 ± 37*	884 ± 44	34.7 ± 3.6*,**
Axotomy			
H46R (n = 5)	751 ± 19	843 ± 23	89.2 ± 1.4
NL (G93A) (n = 6)	743 ± 15	835 ± 12	88.9 ± 0.6
G93A (n = 5)	741 ± 42	781 ± 45	94.9 ± 1.2

[†]Numbers of facial motoneurons and the percent survival at the ipsilateral (lesion) side relative to the contralateral (control) side 2 weeks after avulsion or axotomy. Results are presented as mean ± SEM. Statistical comparison was done by Mann-Whitney U-test. n = number of animals. NL. nontransgenic littermates.
*$P < 0.01$ vs. NL (H46R) and NL (G93A) rats after avulsion.
**$P < 0.05$ vs. H46R-transgenic rats after avulsion.

postoperation (Fig. 2). In contrast, immunohistochemical examination showed perikaryal accumulation of phosphorylated neurofilaments in injured motoneurons both after axotomy and after avulsion, as described previously (Koliatsos et al., 1989, 1994; Koliatsos and Price, 1996). There were no hyaline inclusions identifiable in HE-stained sections or ubiquitin-immunoreactive structures in both H46R- and G93A-tg rats and their non-tg littermates on either operated or contralateral sides (data not shown). Proliferation of astrocytes as evidenced by immunostaining for GFAP was observed at the injured sides in all the animals after avulsion and axotomy, and the degree of the astrocytic response appeared to correlate with the extent of motoneuron loss after avulsion; i.e., more intense GFAP immunostaining was demonstrated when less neuronal survival was observed (Fig. 3).

It has been shown that ATF3 is expressed, and c-Jun and Hsp27 are up-regulated and phosphorylated, in injured motoneurons after axotomy (Tsujino et al., 2000; Casanovas et al., 2001; Benn et al., 2002; Kalmár et al., 2002). Several reports have documented that ATF3, c-Jun, and Hsp27 cooperate to promote neuronal survival in vitro and in vivo, suggesting neuroprotective roles of these molecules (Pearson et al., 2003; Nakagomi et al., 2003). We then examined the expression of ATF3, c-Jun, and Hsp27 in injured motoneurons after facial nerve avulsion that causes extensive neuronal loss. In wild-type adult rats, intact facial motoneurons were constitutively immunoreactive for c-Jun and Hsp27 but not for ATF3, phosphorylated c-Jun, or phosphorylated Hsp27, whereas injured motoneurons become immunoreactive for ATF3, phosphorylated c-Jun, and phosphorylated Hsp27 within 1 day after facial nerve avulsion and remain positive up to 4 weeks (Watabe et al., unpublished observations). In a similar manner, virtually all injured motoneurons were immunostained for ATF3, phosphorylated c-Jun, and phosphorylated Hsp27 in H46R- and G93A-tg rats and their non-tg littermates 2 weeks after avulsion and axotomy as examined in this study (Fig. 3).

DISCUSSION

We demonstrated that only 50% (H46R-tg rats) or 35% (G93A-tg rats) of motoneurons in mutant SOD1-tg rats survived 2 weeks after avulsion at their presymptomatic stage compared with 70% survival of motoneurons in their non-tg littermates, indicating that motoneuron degeneration after avulsion is significantly more severe in these presymptomatic mutant SOD1-tg rats. It is interesting to note that the loss of motoneurons in G93A-tg rats was significantly greater than that in H46R-tg rats after avulsion, insofar as the onset of paralysis is earlier and the disease progression is more rapid in G93A-tg rats compared with the H46R rats used in the present study (Nagai et al., 2001). The clinical courses of these tg rats are also likely to be relevant to those of human mutant SOD1-mediated familial ALS, in that the human H46R cases progress very slowly compared with the G93A cases (Nagai et al., 2001; Aoki et al., 1993, 1994). In contrast, we did not see significant motoneuron loss in the presymptomatic SOD1-tg rats and their non-tg littermates 2 weeks after facial nerve axotomy. Unlike avulsion, axotomy does not generally induce significant motoneuron death in adult rodents (Lowrie and Vrbová, 1992; Moran and Graeber, 2004), except that, in the case of adult Balb/C mice, the facial nerve axotomy leads to loss of >50% of the motoneurons at 30 days postoperation (Hottinger et al., 2000), and C57BL mice show late motoneuron loss (~60%) 8 weeks after facial nerve axotomy (Angelov et al., 2003). Mariotti et al. (2002) axotomized facial nerves of G93A-tg mice and their non-tg littermates at their presymptomatic stage and observed loss of facial motoneurons that was higher in G93A-tg mice than in non-tg littermates at 30 days postaxotomy; these data are relevant to our present data acquired from avulsion, but not axotomy, in rats, which probably is due to the use of different animal species. In contrast, Kong and Xu (1999) described axotomy of lumbar spinal or sciatic nerve in G93A-tg mice at the presymptomatic stage reducing the extent of axon degeneration at the end stage of the disease. They did

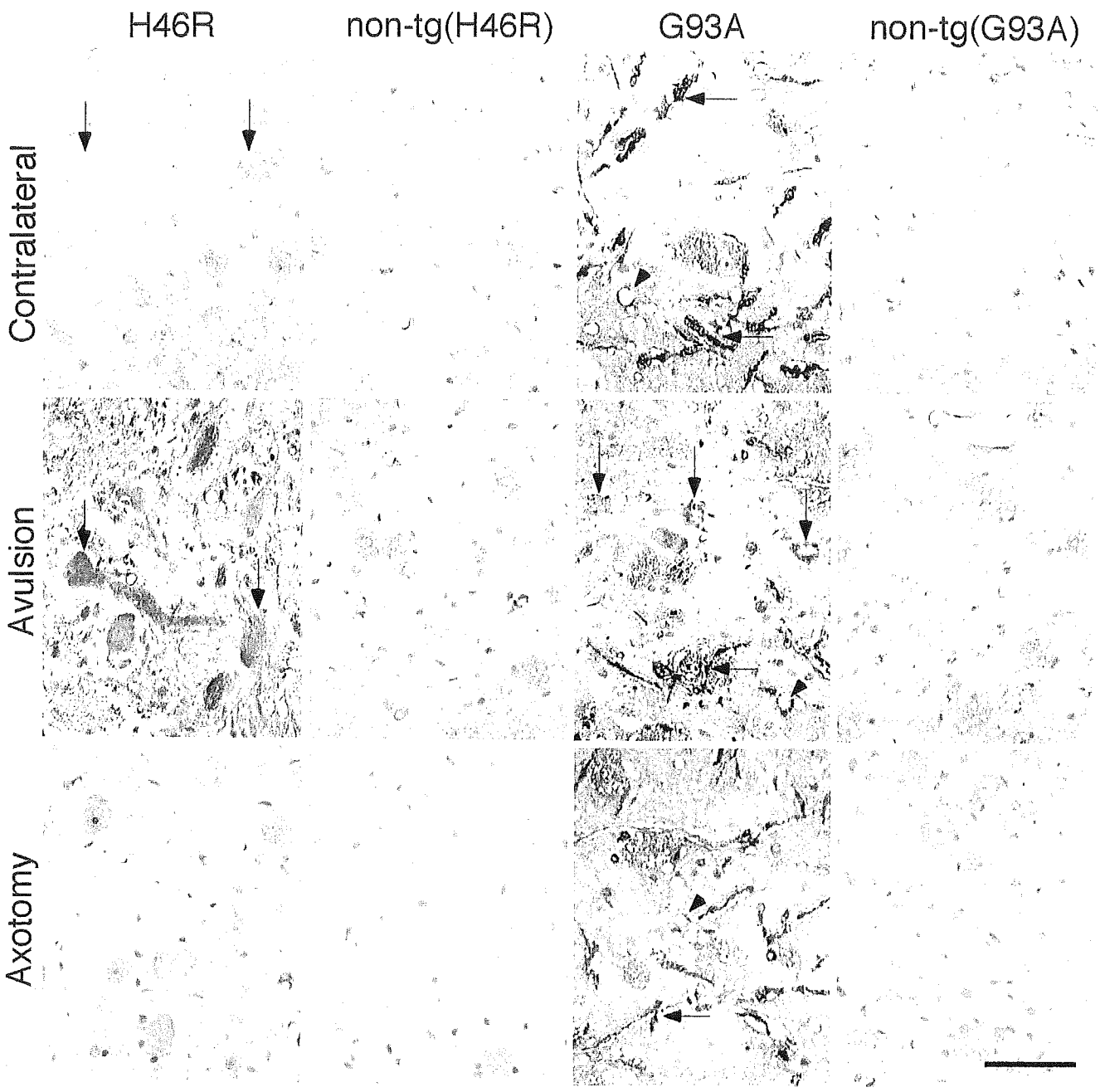

Fig. 2. SOD1 immunohistochemistry of facial motoneurons of H46R- and G93A-tg rats and their non-tg littermates on the contralateral and ipsilateral (avulsion or axotomy) sides 2 weeks after facial nerve avulsion or axotomy. Counterstained with hematoxylin. Note immunostained motoneurons (vertical arrows), axons (horizontal arrows), and vacuoles in neuropil (arrowheads) in H46R- and G93A-tg rats. Scale bar = 50 μm.

not evaluate the response of the cell bodies of spinal motoneurons, so it remains unknown whether SOD1 mutation affects the viability of spinal motoneurons after axotomy. In the present study, we demonstrated that motoneuron degeneration after facial nerve avulsion, but not after axotomy, is exacerbated in presymptomatic mutant SOD1-tg rats at 2 weeks postoperation. These data clearly indicate the increased vulnerability of facial motoneurons to proximal nerve injury in the presymptomatic SOD1-tg rats.

It has been shown that SOD1 is abundantly expressed in cell bodies, dendrites, and axons of wild-type mouse and rat motoneurons in vivo (Pardo et al., 1995; Moreno et al., 1997; Yu, 2002). In the present

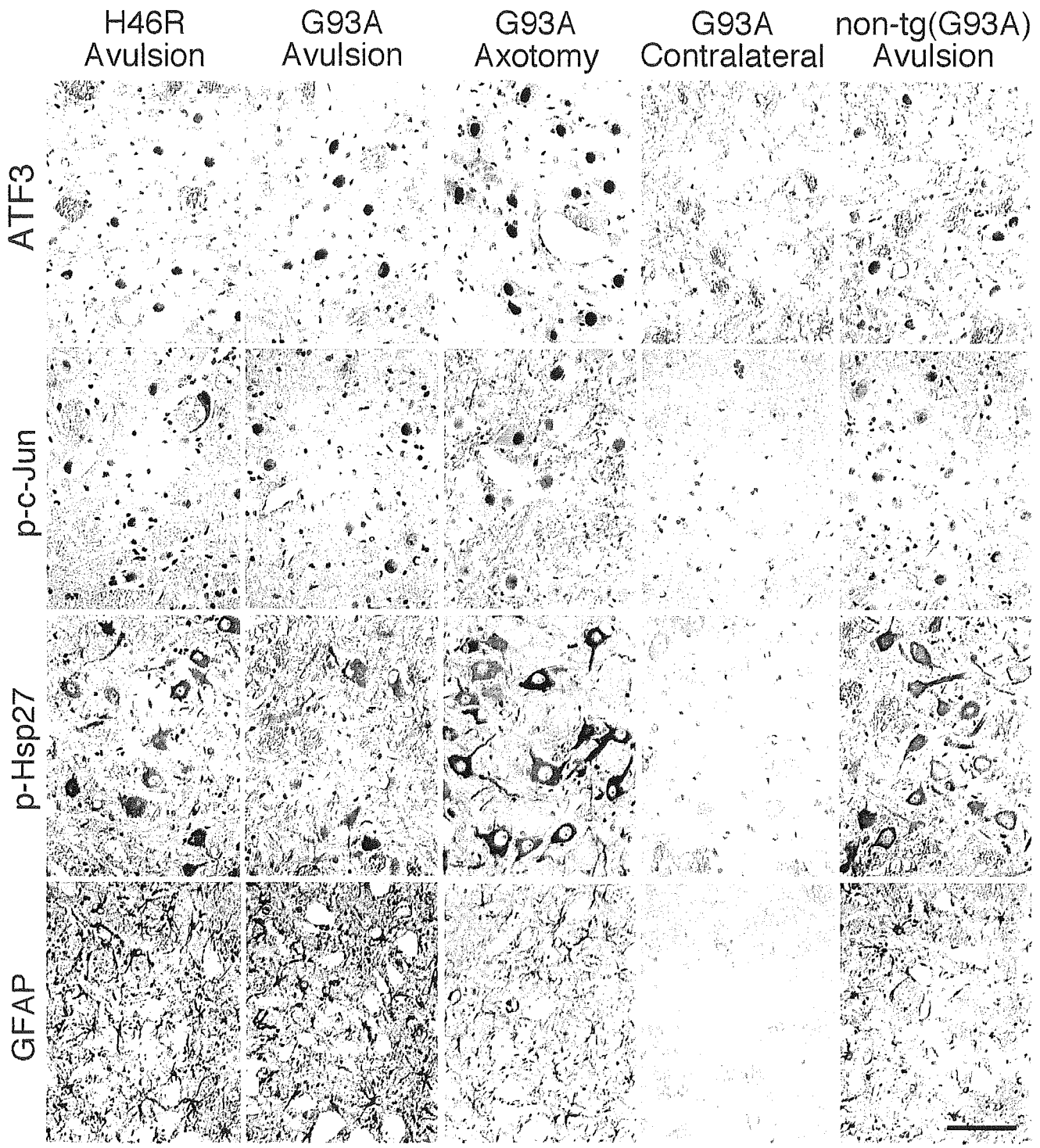

Fig. 3. Immunohistochemistry for ATF3, phosphorylated c-Jun (p-c-Jun), phosphorylated Hsp27 (p-Hsp27), and GFAP of facial nuclei in H46R-tg rat, G93A-tg rat, and non-tg littermate on the ipsilateral (avulsion or axotomy) and contralateral sides 2 weeks after facial nerve avulsion or axotomy. All injured motoneurons are immunostained for ATF3, phosphorylated c-Jun, and phosphorylated Hsp27 in these rats after avulsion or axotomy. The intensity of GFAP immunoreactivity appears parallel to the extent of motoneuron loss (see also Fig. 1). Counterstained with hematoxylin. Scale bar = 50 μm.

study, we did not observe immunoreactivity for SOD1 in facial motoneurons of nontransgenic littermates with sheep and rabbit anti-human SOD1 antibodies; it is postulated that the antibody concentrations (i.e., 1:1,000–10,000) used in this study are below the detection levels for immunostaining rat SOD1 antigen on paraffin sections. Instead, we demonstrated some facial motoneurons showing very faint immunoreactivity for SOD1 in H46R-tg rats on paraffin sections. In G93A-tg rats, axons and vacuoles in neuropil were intensely immunoreactive for SOD1 at both uninjured and injured sides. The increased immunostaining for SOD1 in injured motoneurons of SOD1 (H46R and G93A)-tg rats may therefore indicate that human mutant SOD1 protein is accumulated in the cytoplasm of facial motoneurons after avulsion. When several mutant SOD1 genes that include G93A were transfected to COS7 cells, the mutant SOD1s, but not wild-type SOD1, aggregated in association with the endoplasmic reticulum (ER) and induced ER stress (Tobisawa et al., 2003). Accumulation of mutant SOD1 in injured motoneurons after avulsion may therefore potentiate ER stress and exacerbate motoneuron death in the presymptomatic mutant SOD1-tg rats, although the mechanism of accumulation of SOD1 remains unknown. Whether up-regulation of cytoplasmic mutant SOD1 expression or retrograde accumulation of mutant SOD1 from injured axons was induced in these neurons awaits further investigations. In addition, facial nerve axotomy, as opposed to avulsion, did not increase immunoreactivity for SOD1 in injured motoneurons of SOD1-tg rats and their non-tg littermates, which seems consistent with the absence of significant motoneuron loss in these rats as described above. As for wild-type SOD1, previous reports documented no change in SOD1 mRNA levels or SOD1 immunoreactivity in injured motoneurons after facial or sciatic nerve axotomy in wild-type rats (Yoneda et al., 1992; Rosefeld et al., 1997).

It has been demonstrated that ATF3 is expressed, and c-Jun and Hsp27 are up-regulated and phosphorylated, in injured adult motoneurons after axotomy (Tsujino et al., 2000; Casanovas et al., 2001; Benn et al., 2002; Kalmár et al., 2002). As for the neuroprotective nature of these molecules, it has been reported that ATF3 enhances c-Jun-mediated neurite sprouting in PC12 and Neuro-2a cells (Pearson et al., 2003), and ATF3 and Hsp27 cooperate with c-Jun to prevent death of PC12 cells and superior cervical ganglion neurons (Nakagomi et al., 2003). Hsp27 is induced and phosphorylated in adult, but not in neonatal, motoneurons after axotomy, and axotomized neonatal motoneurons that lack Hsp27 die by apoptosis, suggesting that phosphorylated Hsp27 is necessary for motoneuron survival after peripheral nerve injury (Benn et al., 2002). However, there have been no reports concerning the expression of ATF3, phosphorylated c-Jun, and phosphorylated Hsp27 in injured motoneurons after avulsion. In the present study, we have demonstrated that, even after avulsion that causes extensive motoneuron death, ATF3, phosphorylated c-Jun, and phosphorylated Hsp27 were fully up-regulated in both SOD1-tg and non-tg rats. These results suggest that neuroprotective effects of Hsp27 cannot overcome yet unidentified stress(es) induced by facial nerve avulsion. On the other hand, a recent report demonstrated that facial motoneurons of c-Jun-deficient mice are resistant to axotomy-induced cell death, suggesting that c-Jun promotes posttraumatic motoneuron death (Raivich et al., 2004). In addition, it has been shown that mutant SOD1 binds to Hsp27 and forms aggregates, suggesting that this binding of Hsp27 to mutant SOD1 blocks antiapoptotic function of Hsp27 and leads to motoneuron death (Okado-Matsumoto and Fridovich, 2002). The effects of phosphorylated c-Jun and Hsp27 and their association with mutant SOD1 accumulation should be further investigated to elucidate the mechanism of exacerbated motoneuron death in SOD1-tg rats after avulsion.

In this study, we have demonstrated that motoneuron degeneration after facial nerve avulsion is exacerbated in presymptomatic mutant SOD1-tg rats compared with their non-tg littermates. Mutant SOD1 accumulation and its association with c-Jun and Hsp27 may have a key role leading to enhanced motoneuron death. In this context, motoneuron death after avulsion may share, at least in part, a common mechanism with the motoneuron degeneration associated with SOD1 mutation.

ACKNOWLEDGMENT

We are grateful to Dr. Kohtaro Asayama (University of Occupational and Environmental Health, Japan) for kindly providing rabbit anti-SOD1 antibody.

REFERENCES

Angelov DN, Waibel S, Guntinas-Lichius O, Lenzen M, Neiss WF, Tomov TL, Yoles E, Kipnis J, Schori H, Reuter A, Ludolph A, Schwartz M. 2003. Therapeutic vaccine for acute and chronic motor neuron diseases: implications for amyotrophic lateral sclerosis. Proc Natl Acad Sci U S A 100:4790–4795.

Aoki M, Ogasawara M, Matsubara Y, Narisawa K, Nakamura S, Itoyama Y, Abe K. 1993. Mild ALS in Japan associated with novel SOD mutation. Nat Genet 5:323–324.

Aoki M, Ogasawara M, Matsubara Y, Narisawa K, Nakamura S, Itoyama Y, Abe K. 1994. Familial amyotrophic lateral sclerosis (ALS) in Japan associated with H46R mutation in Cu/Zn superoxide dismutase gene: a possible new subtype of familial ALS. J Neurol Sci 126:77–83.

Asayama K, Burr IM. 1984. Joint purification of mangano and copper/zinc superoxide dismutase from a single source: a simplified method. Anal Biochem 136:336–339.

Benn SC, Perrelet D, Kato AC, Scholz J, Decosterd I, Mannion RJ, Bakowska JC, Woolf CJ. 2002. Hsp27 upregulation and phosphorylation is required for injured sensory and motor neuron survival. Neuron 36:45–56.

Casanovas A, Ribera J, Hager G, Kreutzberg GW, Esquerda JE. 2001. c-Jun regulation in rat neonatal motoneurons postaxotomy. J Neurosci 63:469–479.

Cleveland DW. 1999. From Charcot to SOD1: mechanisms of selective motor neuron death in ALS. Neuron 24:515–520.

Cleveland DW, Rothstein JD. 2001. From Charcot to Lou Gehrig: deciphering selective motor neuron death in ALS. Nat Rev Neurosci 2:806–819.

Estévez AG, Spear N, Manuel SM, Barbeito L, Radi R, Beckman JS. 1998. Role of endogenous nitric oxide and peroxynitrite formation in the survival and death of motor neurons in culture. Prog Brain Res 18: 269–280.

Hottinger AF, Azzouz M, Déglon N, Aebischer P, Zurn AD. 2000. Complete and long-term rescue of lesioned adult motoneurons by lentiviral-mediated expression of glial cell line-derived neurotrophic factor in the facial nucleus. J Neurosci 20:5587–5593.

Ikeda K, Sakamoto T, Kawazoe Y, Marubuchi S, Nakagawa M, Ono S, Terashima N, Kinoshita M, Iwasaki Y, Watabe K. 2003. Oral administration of a neuroprotective compound T-588 prevents motoneuron degeneration after facial nerve avulsion in adult rats. Amyotroph Lateral Scler Other Motor Neuron Disord 4:74–80.

Kalmár B, Burnstock G, Vrborá G, Greensmith L. 2002. The effect of neonatal injury on the expression of heat shock proteins in developing rat motoneurons. J Neurotrauma 19:667–679.

Koliatsos VE, Price DL. 1996. Axotomy as an experimental model of neuronal injury and cell death. Brain Pathol 6:447–465.

Koliatsos VE, Applegate MD, Kitt CA, Walker LC, DeLong MR, Price DL. 1989. Aberrant phosphorylation of neurofilaments accompanies transmitter-related changes in rat septal neurons following transection of the fimbria-fornix. Brain Res 482:205–218.

Koliatsos VE, Price WL, Pardo CA, Price DL. 1994. Ventral root avulsion: an experimental model of death of adult motor neurons. J Comp Neurol 342:35–44.

Kong J, Xu Z. 1999. Peripheral axotomy slows motoneuron degeneration in a transgenic mouse line expressing mutant SOD1 G93A. J Comp Neurol 412:373–380.

Lowrie MB, Vrbová G. 1992. Dependence of postnatal motoneurones on their targets: review and hypothesis. Trend Neurosci 15:80–84.

Mariotti R, Cristino L, Bressan C, Boscolo B, Bentivoglio M. 2002. Altered reaction of facial motoneurons to axonal damage in the presymptomatic phase of a murine model of familial amyotrophic lateral sclerosis. Neuroscience 115:331–335.

Martin LJ, Kaiser A, Price AC. 1999. Motor neuron degeneration after nerve avulsion in adult evolves with oxidative stress and is apoptosis. J Neurobiol 40:185–201.

Moran LB, Graeber MB. 2004. The facial nerve axotomy model. Brain Res Rev 44:154–178.

Moreno S, Nardacci R, Ceru MP. 1997. Regional and ultrastructural immunolocalization of copper-zinc superoxide dismutase in rat central nervous system. J Histochem Cytochem 45:1611–1633.

Nagai M, Aoki M, Miyoshi I, Kato M, Pasinelli P, Kasai N, Brown RH Jr, Itoyama Y. 2001. Rats expressing human cytosolic copper-zinc superoxide dismutase transgenes with amyotrophic lateral sclerosis: associated mutations develop motor neuron disease. J Neurosci 21:9246–9254.

Nakagomi S, Suzuki Y, Namikawa K, Kiryu-Seo S, Kiyama H. 2003. Expression of the activating transcription factor 3 prevents c-Jun N-terminal kinase-induced neuronal death by promoting heat shock protein 27 expression and Akt activation. J Neurosci 23:5187–5196.

Okado-Matsumoto A, Fridovich I. 2002. Amyotrophic lateral sclerosis: a proposed mechanism. Proc Natl Acad Sci U S A 99:9010–9014.

Pardo CA, Xu Z, Borchelt DR, Price DL, Sisodia SS, Cleveland DW. 1995. Superoxide dismutase is an abundant component in cell bodies, dendrites, and axons of motor neurons and in a subset of other neurons. Proc Natl Acad Sci U S A 92:954–958.

Pearson AG, Gray CW, Pearson JF, Greenwood JM, During MJ, Dragunow M. 2003. ATF3 enhances c-Jun-mediated neurite sprouting. Brain Res Mol Brain Res 120:38–45.

Raivich G, Bohatschek M, Da Costa C, Iwata O, Galiano M, Hristova M, Nateri AS, Makwana M, Riera-Sans L, Wolfer DP, Lipp HP, Aguzzi A, Wagner EF, Behrens A. 2004. The AP-1 transcription factor c-Jun is required for efficient axonal regeneration. Neuron 43:57–67.

Rosenfeld J, Cook S, James R. 1997. Expression of superoxide dismutase following axotomy. Exp Neurol 147:37–47.

Sakamoto T, Watabe K, Ohashi T, Kawazoe Y, Oyanagi K, Inoue K, Eto Y. 2000. Adenoviral vector-mediated GDNF gene transfer prevents death of adult facial motoneurons. Neuroreport 11:1857–1860.

Sakamoto T, Kawazoe Y, Shen J-S, Takeda Y, Arakawa Y, Ogawa J, Oyanagi K, Ohashi T, Watanabe K, Inoue K, Eto Y, Watabe K. 2003a. Adenoviral gene transfer of GDNF, BDNF and TGFβ2, but not CNTF, cardiotrophin-1 or IGF1, protects injured adult motoneurons after facial nerve avulsion. J Neurosci Res 72:54–64.

Sakamoto T, Kawazoe Y, Uchida Y, Hozumi I, Inuzuka T, Watabe K. 2003b. Growth inhibitory factor prevents degeneration of injured adult rat motoneurons. Neuroreport 14:2147–2151.

Søreide AJ. 1981. Variations in the axon reaction after different types of nerve lesion. Acta Anat 110:173–188.

Tobisawa S, Hozumi Y, Arawaka S, Koyama S, Wada M, Nagai M, Aoki M, Itoyama Y, Goto K, Kato T. 2003. Mutant SOD1 linked to familial amyotrophic lateral sclerosis, but not wild-type SOD1, induces ER stress in COS7 cells and transgenic mice. Biochem Biophys Res Commun 303:496–503.

Tsujino H, Kondo E, Fukuoka T, Dai Y, Tokunaga A, Miki K, Yonenobu K, Ochi T, Noguchi K. 2000. Activating transcription factor 3 (ATF3) induction by axotomy in sensory and motoneurons: a novel neuronal marker of nerve injury. Mol Cell Neurosci 15:170–182.

Watabe K, Ohashi T, Sakamoto T, Kawazoe Y, Takeshima T, Oyanagi K, Inoue K, Eto Y, Kim SU. 2000. Rescue of lesioned adult rat spinal motoneurons by adenoviral gene transfer of glial cell line-derived neurotrophic factor. J Neurosci Res 60:511–519.

Wu W. 1993. Expression of nitric-oxide synthase (NOS) in injured CNS neurons as shown by NADPH diaphorase histochemistry. Exp Neurol 120:153–159.

Yoneda T, Inagaki S, Hayashi Y, Nomura T, Takagi H. 1992. Differential regulation of manganese and copper/zinc superoxide dismutases by the facial nerve transection. Brain Res 582:342–345.

Yu WHA. 2002. Spatial and temporal correlation of nitric oxide synthase expression with CuZn-superoxide dismutase reduction in motor neurons following axotomy. Ann N Y Acad Sci 962:111–121.

WILEY InterScience® DISCOVER SOMETHING GREAT

Journal of Neuroscience Research 83:119–133 (2006)

Disease Progression of Human SOD1 (G93A) Transgenic ALS Model Rats

Arifumi Matsumoto,[1,3,6] Yohei Okada,[1,4,6] Masanori Nakamichi,[5] Masaya Nakamura,[2] Yoshiaki Toyama,[2] Gen Sobue,[4] Makiko Nagai,[3] Masashi Aoki,[3] Yasuto Itoyama,[3] and Hideyuki Okano[1,6]*

[1]Department of Physiology, Keio University School of Medicine, Tokyo, Japan
[2]Department of Orthopaedic Surgery, Keio University School of Medicine, Tokyo, Japan
[3]Department of Neurology, Tohoku University Graduate School of Medicine, Sendai, Japan
[4]Department of Neurology, Nagoya University Graduate School of Medicine, Nagoya, Japan
[5]Takeda Chemical Industries, Ltd., Osaka, Japan
[6]Core Research for Evolutional Science and Technology (CREST), Japan Science and Technology Agency (JST), Saitama, Japan

The recent development of a rat model of amyotrophic lateral sclerosis (ALS) in which the rats harbor a mutated human SOD1 (G93A) gene has greatly expanded the range of potential experiments, because the rats' large size permits biochemical analyses and therapeutic trials, such as the intrathecal injection of new drugs and stem cell transplantation. The precise nature of this disease model remains unclear. We described three disease phenotypes: the forelimb-, hindlimb-, and general-types. We also established a simple, non-invasive, and objective evaluation system using the body weight, inclined plane test, cage activity, automated motion analysis system (SCANET), and righting reflex. Moreover, we created a novel scale, the Motor score, which can be used with any phenotype and does not require special apparatuses. With these methods, we uniformly and quantitatively assessed the onset, progression, and disease duration, and clearly presented the variable clinical course of this model; disease progression after the onset was more aggressive in the forelimb-type than in the hindlimb-type. More importantly, the disease stages defined by our evaluation system correlated well with the loss of spinal motor neurons. In particular, the onset of muscle weakness coincided with the loss of approximately 50% of spinal motor neurons. This study should provide a valuable tool for future experiments to test potential ALS therapies.

Key words: amyotrophic lateral sclerosis; evaluation system; behavioral analyses; phenotype; variability

Amyotrophic lateral sclerosis (ALS) is a fatal neurodegenerative disorder that mainly affects the upper and lower motor neurons (de Belleroche et al., 1995). It is characterized by progressive muscle weakness, amyotrophy, and death from respiratory paralysis, usually within 3–5 years of onset (Brown 1995). Although most cases of ALS are sporadic (SALS), approximately 10% are familial (FALS) (Mulder et al., 1986). Moreover, 20–25% of FALS cases are due to mutations in the gene encoding copper-zinc superoxide dismutase (SOD1) (Deng et al., 1993; Rosen et al., 1993). More than 100 different mutations in the SOD1 gene have been identified in FALS so far.

Until recently, animal models of FALS have been various transgenic mice that express a mutant human SOD1 (hSOD1) gene. Of these, a transgenic mouse carrying the G93A (Gly-93 → Ala) mutant hSOD1 gene was the first described (Gurney et al., 1994) and is used all over the world because this model closely recapitulates the clinical and histopathological features of the human disease. To evaluate the therapeutic effects of potential ALS treatments in this animal, many motor-related behavioral tasks are used (Chiu et al., 1995; Barneoud et al., 1997; Garbuzova-Davis et al., 2002; Sun et al., 2002; Wang et al., 2002; Inoue et al., 2003; Kaspar et al., 2003; Weydt et al., 2003; Azzouz et al., 2004). However, transgenic mice have innate limitations for some types of experiments because of their small size.

Recently, transgenic rat models of ALS, which harbor the hSOD1 gene containing the H46R (His-46 → Arg) or G93A mutation were generated (Nagai et al., 2001). The larger size of these rat models makes certain experiments easier, such as biochemical analyses that require large amounts of sample, intrathecal administration

Contract grant sponsor: Core Research for Evolutional Science and Technology (CREST), Japan Science and Technology Agency (JST); Contract grant sponsor: Japanese Ministry of Health, Labour and Welfare; Contract grant sponsor: Japanese Ministry of Education, Culture, Sports, Science and Technology.

*Correspondence to: Hideyuki Okano, Department of Physiology, School of Medicine, Keio University, 35 Shinanomachi, Shinjuku-ku, Tokyo, 160-8582, Japan. E-mail: hidokano@sc.itc.keio.ac.jp

Received 22 August 2005; Revised 29 September 2005; Accepted 30 September 2005

Published online 7 December 2005 in Wiley InterScience (www.interscience.wiley.com). DOI: 10.1002/jnr.20708

of drugs, and, especially, therapeutic trials, including the transplantation of neural stem cells into the spinal cord. The hSOD1 (G93A) transgenic rats typically present weakness in one hindlimb first. Later, weakness progresses to the other hindlimb and to the forelimbs. Finally, the rats usually become unable to eat or drink, and eventually die. Only subjective and ambiguous analyses were made with regard to the clinical progression of this ALS animal model and objective criteria for evaluating the efficacy of these new treatments have not been determined. For these reasons, we assessed the disease progression quantitatively using five different measures (body weight, inclined plane test, cage activity, SCANET, and righting reflex) and established an easy, noninvasive, and objective evaluation system that is sensitive to small but important abnormalities in the hSOD1 (G93A) transgenic rats. In addition, we created a novel scale, the Motor score, to assess disease progression in the transgenic rats without using special apparatuses. We also examined the validity of these measures as assessment tools for the pathology by investigating the number of spinal motor neurons remaining at the disease stages defined by each measure.

MATERIALS AND METHODS

Transgenic Rats

All animal experiments were conducted according to the Guidelines for the Care and Use of Laboratory Animals of Keio University School of Medicine. We used hSOD1 (G93A) transgenic male rats (Nagai et al., 2001) from our colony and their age- and gender-matched wild-type littermates as controls. Rats were housed in a specific pathogen-free animal facility at a room temperature of 23 ± 1°C under a 12-hr light-dark cycle (light on at 08:00). Food (solid feed CE-2, 30kGy; CLEA Japan, Inc.) and water were available ad lib. Transgenic rats were bred and maintained as hemizygotes by mating transgenic males with wild-type females. Transgenic progeny were identified by detecting the exogenous hSOD1 transgene, by amplification of pup tail DNA extracted at 20 days of age by polymerase chain reaction (PCR). The primers and cycling conditions were described previously (Nagai et al., 2001).

Exploration of Assessment Tools to Measure Disease Progression in the hSOD1 (G93A) Transgenic Rats

We evaluated the usefulness of four different measures to assess disease progression in the transgenic rats. All tests were carried out between 12:00–16:00 and in a double-blind fashion.

Body weight. Animals ($n = 9$ for each genotype) were weighed weekly after 30 days of age with an electronic scale. To avoid overlooking the beginning of weight loss, the animals were weighed every second or third day after 90 days of age, the age at which motor neurons are reported to be lost in the lumbar spinal cord (Nagai et al., 2001).

Inclined plane. This test was initially established mainly to assess the total strength of the forelimbs and hindlimbs in a model of spinal cord injury (Rivlin and Tator, 1977). Briefly, rats were placed laterally against the long axis of the inclined plane, and the maximum angle at which they could maintain their position on the plane for 5 sec was measured. To assess the strength of both sides of limbs equally, animals were placed on the inclined plane with the right side of the body to the downhill side of the incline, and then with the left side of the body facing downhill. For each rat, the test was carried out three times for each side, and the mean value of the angles obtained for the right side was compared to that obtained for the left. The lower mean value was recorded as the angle for that rat. Animals ($n = 9$ for each genotype) were tested weekly after 70 days of age and every second to third day after 100 days of age.

Cage activity. Animals ($n = 8$ for each genotype) were housed individually and monitored every day for all 24 hr (except for the days the cages were changed) after they were 70 days old. Spontaneous locomotor activity in the home cage (345 × 403 × 177 mm) was recorded by an activity-monitoring system (NS-AS01; Neuroscience, Inc., Tokyo, Japan) as described previously (Ohki-Hamazaki et al., 1999). The sensor detects the movement of animals using the released infrared radiation associated with their body temperature. The data were analyzed by the DAS-008 software (Neuroscience, Inc., Tokyo, Japan). To eliminate data variability owing to differences in the baseline movement of each rat, the baseline value was calculated as the mean of movement from 70–90 days of age, during which all rats were considered to move normally. We analyzed the data at each time point as the percentage of the baseline value in defining disease onset with this test.

SCANET. For short-term activity, 10 min of spontaneous activity was measured with the automated motion analysis system SCANET MV-10 (Toyo Sangyo Co., Ltd., Toyama, Japan) (Mikami et al., 2002). Animals ($n = 4$ for each genotype) were tested weekly after 30 days of age and every second or third day after 100 days of age. Each rat was individually placed in the SCANET cage for 10 min. Three parameters were measured: small horizontal movements of 12 mm or more (Move 1; M1), large horizontal movements of 60 mm or more (Move 2; M2), and the frequency of vertical movements caused by rearing (RG). To distinguish RG movements from incomplete standing actions, the upper sensor frame was adjusted to 13 cm above the lower sensor frame.

Righting reflex. All affected animals were tested for the ability to right themselves within 30 sec of being turned on either side (righting reflex) (Gale et al., 1985). Failure was seen when animals reached the end-stage of disease (Howland et al., 2002), and was regarded as a generalized loss of motor activity. We used this time point, which we call "end-stage," as "death" rather than the actual death of the animal, to exclude the influence of poor food intake and respiratory muscle paralysis on the survival period. All end-stage animals were sacrificed after being deeply anesthetized.

All statistical analyses were carried out with the two-tailed unpaired Student's t-test. A P-value of <0.05 was considered statistically significant.

Motor Score

To establish our own scoring system for motor function, which could be uniformly applicable to any disease phenotype of this rat model, we examined the common clinical findings

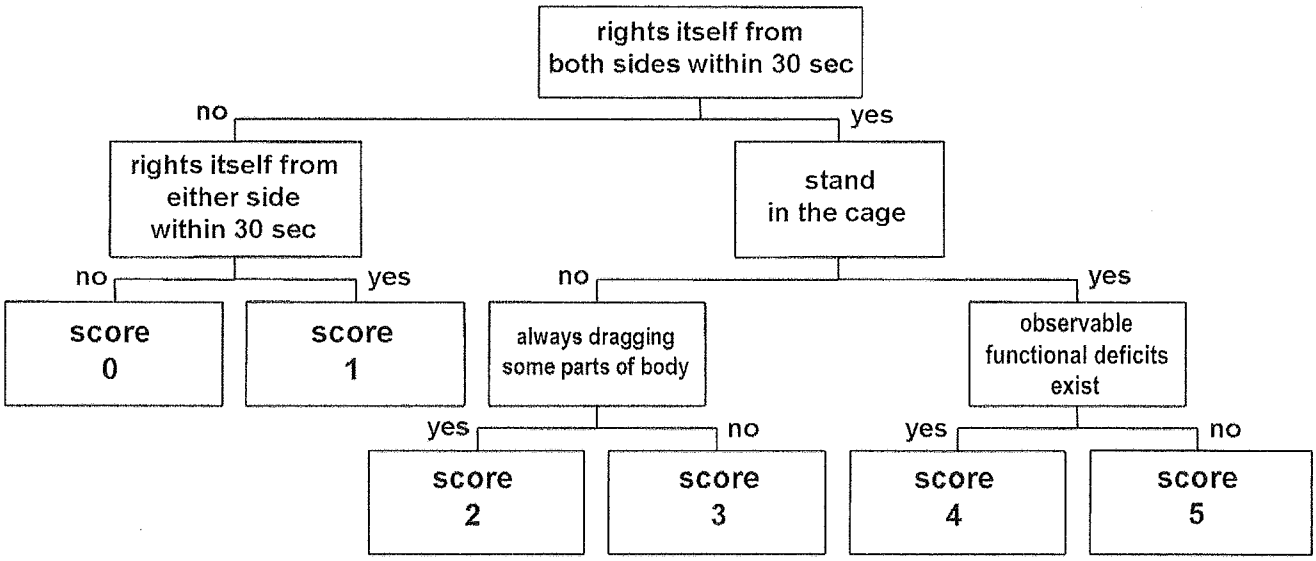

Fig. 1. Chart of Motor score assessment. The degree of motor dysfunction can be assessed by the Motor score as shown in this chart. This scoring system is meant to be used after disease onset, which can be prospectively diagnosed by the inclined plane test (muscle weakness onset). A score of 4 means the same condition as seen for subjective onset (SO). Rats with a score of 5 seem almost as normal as wild-type rats. The detailed testing procedure for the Motor score is described in the text.

of the transgenic rats in detail and assessed their motor functions (n = 20). We focused on the following tests: the righting reflex, the ability to stand in the cage, the extent of dragging their bodies when moving, and the existence of observable functional deficits. We evaluated these items sequentially along with the disease progression and classified the rats into six groups by giving them scores between 0 and 5. The scoring chart (Motor score) is shown in Figure 1.

When disease onset in the rats was diagnosed by their scoring <70° on the inclined plane test (muscle weakness onset), the affected rats were tested for righting reflex. If they were unable to right themselves from either side, they were given a score of 0. If they could right themselves from only one side but not the other, they were given a score of 1.

Rats that could right themselves from both sides were examined for the ability to stand in the cage as follows: Rats were observed in the home cage for 1 min to see if they would stand spontaneously (Step 1). When they moved little in the home cage or showed no tendency to stand during Step 1, they were stimulated by being transferred to another cage (Step 2), and then by being returned to their home cage again (Step 3); the transfers were done to activate exploration motivation. During Step 3, the rats were further stimulated by lightly knocking the cage to intensify the motivation to explore. Each step was carried out for 1 min and the test was stopped when the rat stood once. Rats were judged as "unable to stand" if they did not stand, even after all three steps.

Rats that did not stand were subjected to the next test in the open field, where the extent to which they dragged their bodies when moving was assessed. Those who always dragged and could not lift some parts of their bodies except for scrotums and tails at any time were given a score of 2. If they could lift their dragging parts off the ground for even a moment, they were given a score of 3. The phenotype of dragging the forelimbs was different from that of dragging the hindlimbs. As disease progressed, "forelimb-type" rats first began to touch the tips of their noses on the ground, and then began to drag their head and upper trunk as they moved backward with their hindlimbs. "Hindlimb-type" rats dragged their lower trunk and moved forward with their forelimbs.

Finally, rats that had no abnormality in the above-mentioned assessments were examined in detail to see whether they had any observable functional deficits such as paralysis of the limbs or symptoms of general muscle weakness (e.g., walking with a limp, sluggish movement) in the open field. This condition could be judged subjectively and was defined as subjective onset. Rats with any of these symptoms were given a score of 4; otherwise they were given a score of 5.

Because the scores were based on subjective judgment, they might vary depending on the examiner. To examine inter-rater variability, three transgenic rats of different clinical types were examined according to the method described above, recorded on video tape, and subsequently scored by five observers from different backgrounds (Table I). The scores classified by the five observers were statistically analyzed for inter-rater agreement using Cohen's κ statistics (Table II). Kappa values can range from 0 (no agreement) to 1.00 (perfect agreement), and can be interpreted as poor (<0.00), slight (0.00–0.20), fair (0.21–0.40), moderate (0.41–0.60), substantial (0.61–0.80), and almost perfect (0.81–1.00) (Landis and Koch, 1977). The scores for the three transgenic rats were, on the whole, quite consistent among the five observers, suggesting that the Motor score can be used as an objective method for assessing disease progression.

TABLE I. Motor Score of Transgenic Rats Assessed by Five Different Observers

Transgenic rat	Observer	Days after onset (days) 0	1	2	3	4	5	6	7	8
#1407 Eventual hindlimb type										
	A	5	4	4		2	2	1	0	
	B	4	4	4		2	2	1	0	
	C	4	4	4		2	2	1	0	
	D	4	4	4		2	2	1	0	
	E	4	4	4		2	2	1	0	
	Mean	4.2	4	4		2	2	1	0	
#1470 Pure hindlimb type										
	A	5		4	4	2	2	2	2	0
	B	5		4	3	3	2	2	2	0
	C	5		4	3	2	2	2	2	0
	D	4		4	4	2	2	2	2	0
	E	4		4	3	2	2	2	2	0
	Mean	4.6		4	3.4	2.2	2	2	2	0
#1449 Pure forelimb type										
	A	4	3	3	3		2	1	1	0
	B	4	3	3	3		2	1	1	0
	C	3	3	3	3		2	1	1	0
	D	3	3	3	3		2	1	1	0
	E	4	3	2	2		2	1	1	0
	Mean	3.6	3	2.8	2.8		2	1	1	0

TABLE II. The kappa Statistics for Inter-Rater Agreement of Motor Score

Observers	Transgenic rat (clinical type) #1407 Eventual hindlimb	#1470 Pure hindlimb	#1449 Pure forelimb
A vs. B	0.82	0.69	1.00
A vs. C	0.82	0.82	0.83
A vs. D	0.82	0.81	0.83
A vs. E	0.82	0.70	0.69
B vs. C	1.00	0.83	0.83
B vs. D	1.00	0.53	0.83
B vs. E	1.00	0.66	0.69
C vs. D	1.00	0.64	1.00
C vs. E	1.00	0.82	0.54
D vs. E	1.00	0.81	0.54

TABLE III. Clinical Types of hSOD1 (G93A) Transgenic Rats

Clinical type	Subtype	*n*	%
Forelimb	Pure	4	8.2
	Eventual	5	10.2
Hindlimb	Pure	19	38.7
	Eventual	17	34.7
General		4	8.2
Total		49	100

Real-Time RT-PCR and Western Blot Analysis

Tissue specimens were dissected from the cerebral cortices, cerebella, medullae, and spinal cords (cervical, thoracic, and lumbar spinal cords) of the deeply anesthetized rats, and divided into two portions for total RNA and total protein preparation. Total RNA was isolated and first strand cDNA was synthesized as described previously (Okada et al., 2004). The real time RT-PCR analysis was carried out using Mx3000P (Stratagene, La Jolla, CA) with SYBR Premix Ex Taq (Takara Bio, Inc., Otsu, Japan). The primers used for the analysis were human *SOD1* (5′-TTGGGCAATGTGACTGCTGAC-3′, 5′-AGCTAGCAGGATAACAGATGA-3′), rat *SOD1* (5′-ACTTCGAGCAGAAGGCAAGC-3′, 5′-ACATTGGCCACACCGTCCTTTC-3′), and *β-actin* (5′-CGTGGGCCGCCCTAGGCACCA-3′, 5′-TTGGCCTTAGGGTTCAGAGGGG-3′). The results are presented as ratios of mRNA expression normalized to an inner control gene, *β-actin*. Total protein was prepared in lysis buffer containing 10 mM Tris-HCl (pH 7.6), 50 mM NaCl, 30 mM sodium pyrophosphate, 50 mM sodium fluoride, 20 mM glycerophosphate, 1% Triton X-100, and a protease inhibitor mixture (Complete; Roche Applied Science, Mannheim, Germany). Western blot analysis was carried out by a method established previously. In brief, a 5 μg protein sample of an extract was run on 12% SDS-PAGE, transferred to nitrocellulose, and probed with anti-human SOD1 (1:1,000, mouse IgG, Novocastra Laboratories, Ltd., Benton Lane, UK), and anti-α-tubulin (1:2,000, mouse IgG, Sigma-Aldrich, Inc., Saint Louis, MO). Signals were detected with HRP-conjugated secondary antibodies (Jackson ImmunoResearch Laboratories, Inc., West Grove, PA) using an ECL kit (Amersham Bioscience UK limited, Little Chalfont, UK). Quantitative analysis was carried out with a Scion Image (Scion Corporation, Frederick, MD). The amounts of proteins loaded in each slot were normalized to those of α-tubulin.

Immunohistochemical Analysis

Rats were deeply anesthetized (ketamine 75 mg/kg, xylazine 10 mg/kg, i.p.) and transcardially perfused with 4% paraformaldehyde/PBS (0.1 M PBS, pH 7.4) for histological examination. Spinal cord tissues were dissected out and post-fixed overnight in the same solution. Each spinal cord was dissected into segments that included the C6, T5, and L3 levels, immersed in 15% sucrose/PBS followed by 30% sucrose/PBS at 4°C, and embedded in Tissue-Tek O.C.T. Compound (Sakura Finetechnical Co., Ltd., Tokyo, Japan). Embedded tissue was immediately frozen with liquid nitrogen and stored at −80°C. Serial transverse sections of each spinal segment were cut on a cryostat at a thickness of 14 μm. The sections were pre-treated with acetone for 5 min, rinsed with PBS three times and permeabilized with TBST (Tris-buffered saline with 1% Tween 20) for 15 min at room temperature. After being blocked in the TNB buffer (Perkin-Elmer Life Sciences, Inc., Boston, MA) for 1 hr at room temperature, the sections were incubated at 4°C overnight with an anti-choline acetyltransferase (ChAT) polyclonal antibody (AB144P, Goat IgG, 1:50; Chemicon International, Inc., Temecula, CA). After being washed with PBS three times, the sections were incubated for 2 hr at room temperature with a biotinylated secondary antibody (Jackson ImmunoResearch Laboratories, Inc.). Finally, the labeling was developed using the avidin-biotin-peroxidase complex procedure (Vectastain ABC kits; Vector Laboratories, Inc., Burlingame, CA) with 3,3-diaminobenzidine (DAB; Wako Pure Chemical Industries, Ltd., Osaka, Japan) as the chro-

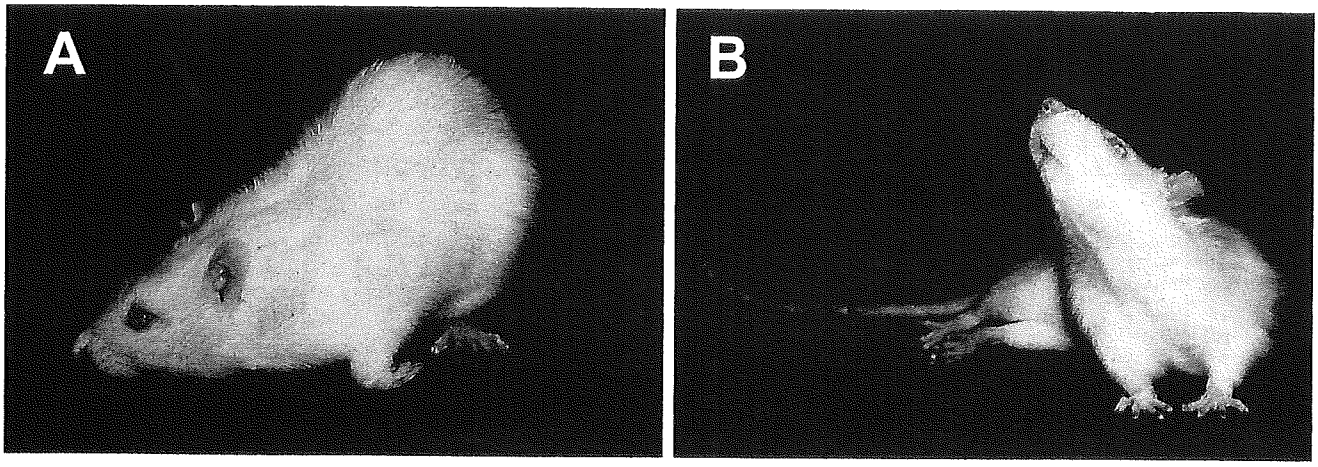

Fig. 2. Characteristic appearance of hSOD1 (G93A) transgenic rats. **A:** Forelimb type. The rat was unable to raise its head and was obligated to take a posture of raising the lumbar region, as indicated, because of the paralyzed forelimbs. **B:** Hindlimb type. The rat showed paraplegia, but was able to raise its head and upper trunk with its non-paralyzed forelimbs.

mogen. Immunohistochemical images were examined with a Zeiss-AxioCam microscope system.

Motor neurons bearing ChAT-immunoreactivity in laminae VII, VIII, and IX of the ventral horn were counted in every tenth section (5 sections total for each segment) for each of the C6, T5, and L3 segments. Only the neurons that showed labeling above background level and were larger than 20 μm in diameter were counted. The numbers of motor neurons in all segments (C6, T5, and L3) were summed for each animal to evaluate not only the local motor neuron loss, but the generalized loss of motor neurons throughout the spinal cord of each animal ($n = 3$ for each genotype at each time point). We next examined the correlation between the number of residual motor neurons and the results of the functional analyses described in this study. Statistical analysis was carried out with two-tailed unpaired Student's *t*-test. A *P*-value of <0.05 was considered statistically significant.

RESULTS

Clinical Types of hSOD1 (G93A) Transgenic Rats

Because we noticed variations in the disease phenotypes expressed by the G93A rats, we classified 49 rats into three clinical categories according to the location of initial paralysis. The clinical types were: the forelimb type, hindlimb type, and general type (Table III). Rats whose paralysis started in the forelimbs and progressed to the hindlimbs were defined as the "forelimb type." In contrast, rats whose paralysis started from the hindlimbs and progressed to the forelimbs were defined as the "hindlimb type." A typical appearance for the forelimb and hindlimb types is shown in Figure 2. Other rats, which showed simultaneous paralysis in the forelimbs and hindlimbs, were categorized as the "general type".

In addition, we classified the forelimb- and hindlimb-type rats into two subtypes, the pure and eventual types, based on the timing of the initial paralysis (Table III). Rats of the pure type showed paralysis that was limited to one or more of the four limbs as the initial observable deficit. Those of the eventual type initially showed symptoms of general muscle weakness (e.g., walking with a limp, sluggish movement), but without unequivocal limb paralysis. In the eventual type animals, paralysis of one of the limbs became apparent later. The ratio of each subtype is shown in Table III.

Evaluation of Disease Progression in the hSOD1 (G93A) Transgenic Rats

Although the transgenic rats varied in their clinical types, all four measures of disease progression (body weight, inclined plane test, cage activity, and SCANET) showed significant differences between the transgenic and wild-type rats (Fig. 3).

In contrast to the continuous weight gain in wild-type rats, the body weight in the affected rats ceased to increase and gradually decreased, with peak body weight attained around 110–120 days of age ($P < 0.05$, after 112 days of age) (Fig. 3A).

In the inclined plane test, initially both the transgenic and wild-type rats uniformly scored 75–80 degrees, after several training trials. However, the transgenic rats showed a significant decline in performance compared to their wild-type littermates from 120 days of age (Fig. 3B).

In the cage activity measurement, the movements of the wild-type rats remained stable, whereas those of the transgenic rats declined rapidly after 125 days of age (Fig. 3C).

In the SCANET test, even the wild-type rats showed decreased movements for all parameters (M1, M2, RG) in the late observation period, though they showed no abnormality in their motor functions. This might be because they had acclimated to the SCANET cage. The movement score of the transgenic rats was consistently worse than that of the wild-type rats after

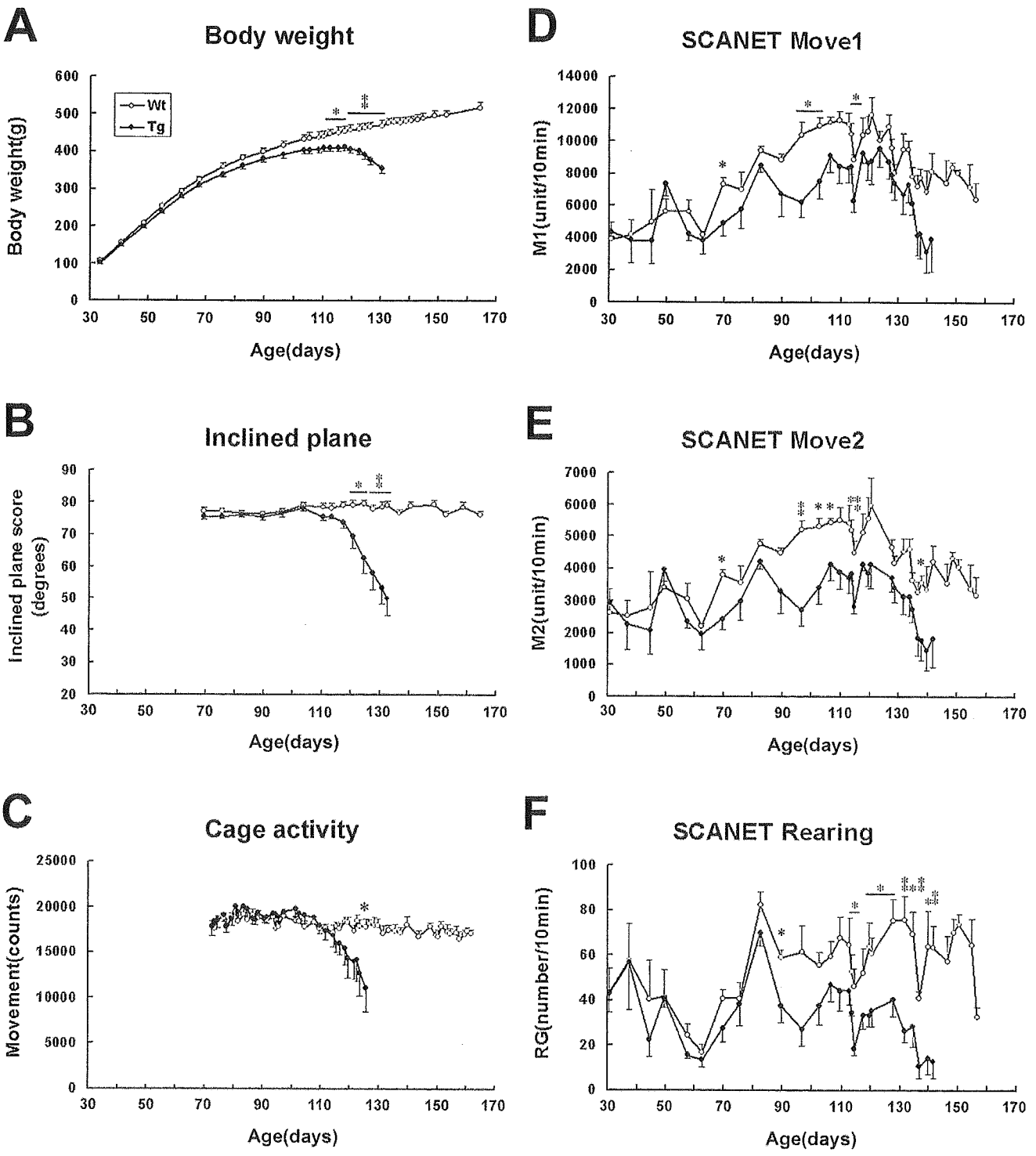

Fig. 3. Disease progression in hSOD1 (G93A) transgenic rats monitored by four effective measures. **A:** Body weight. The weight gain of the transgenic group stopped at around 110–120 days. The difference became statistically significant at 112 days of age ($n = 9$ for each genotype). **B:** Inclined plane. The wild-type group scored 75–80° throughout the period, whereas the score of the transgenic group declined. The difference became statistically significant at 120 days of age ($n = 9$ for each genotype). **C:** Cage activity. The movements of the wild-type group were stable, whereas the scores of the transgenic group declined. Significance was reached at 125 days of age ($n = 8$ for each genotype). **D–F:** SCANET. For all parameters (M1, M2, RG), the movement scores of the transgenic group became constantly worse than those of the wild-type group after 60 days of age. The differences between the groups increased markedly after 90 days of age. Significance was attained beginning at 67 days of age for M1 and M2, and at 87 days of age for RG ($n = 4$ for each genotype). The comparison between the wild-type and transgenic groups was stopped when the first of the transgenic rats reached the end-stage of the disease and was sacrificed. Mean ± SEM. $^*P < 0.05$. $^{**}P < 0.01$; two-tailed unpaired Student's t-test.

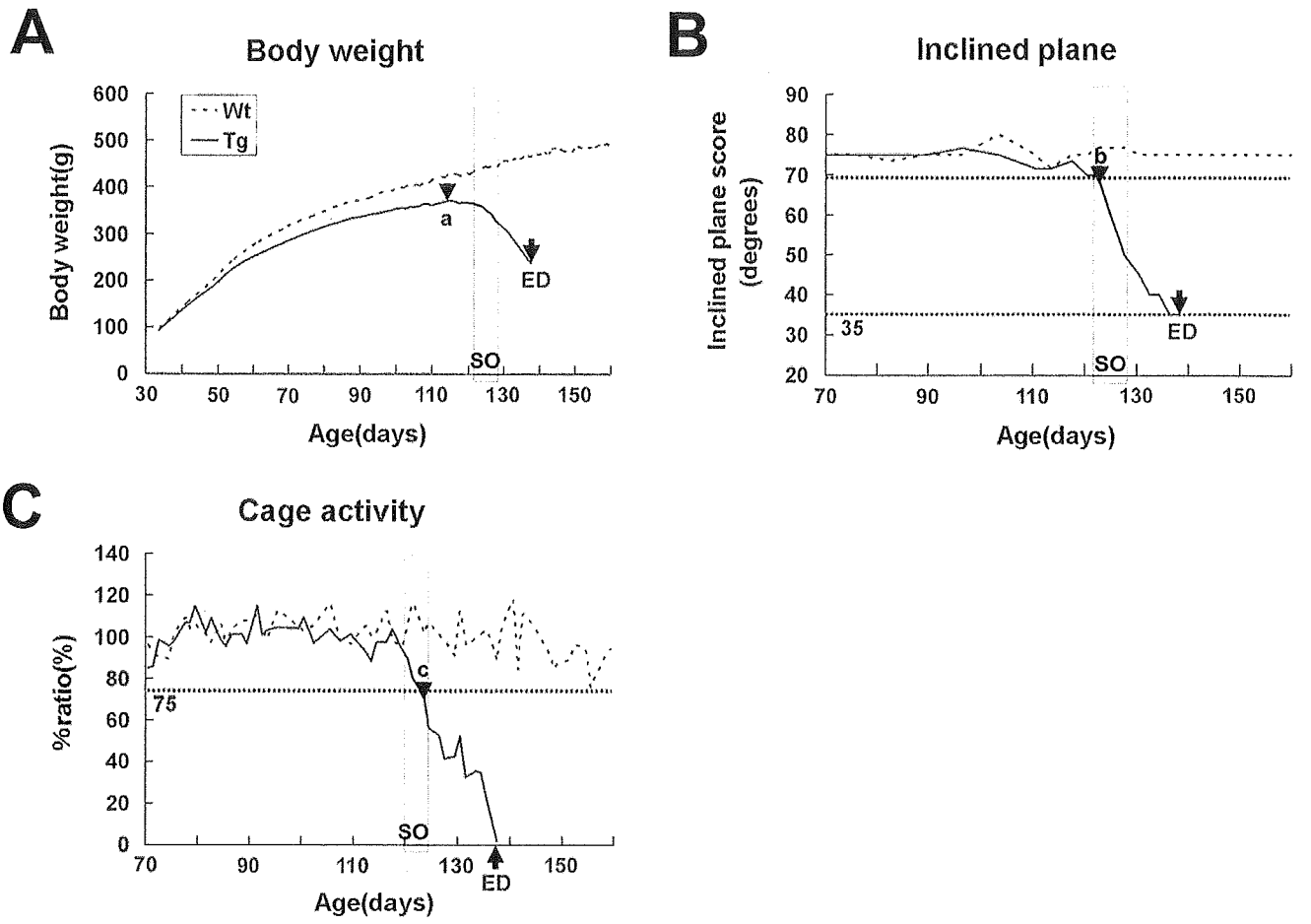

Fig. 4. Schematic presentation of the results from the body weight (**A**), inclined plane test (**B**), and cage activity (**C**) assessments. The onset defined by each measure (black arrowheads) and the end-stage of the disease (ED, black arrows) are indicated in the figures. a, pre-symptomatic onset: the day the transgenic rats scored their maximum body weight. b, muscle weakness onset: the earliest day the transgenic rats scored <70° in the inclined plane test. c, hypo-activity onset: the earliest day the transgenic rats scored <75% of the mean movements from 70–90 days of age in the cage activity measure. SO, subjective onset: the earliest day that observable functional deficits such as paralysis of the limbs or symptoms of general muscle weakness were observed subjectively in the open field (the gray shaded region in A–C).

60 days of age for all parameters (M1, M2, RG), however, even after the wild-type animals showed the decrease in their movement scores. The differences between the two groups increased markedly after 90 days of age for M1, M2, and RG (Fig. 3D–F). The performance of each rat fluctuated so markedly that the SCANET test seems to be inappropriate for statistical analysis.

Onset, End-Stage, and Duration of Disease in hSOD1 (G93A) Transgenic Rats

Using the quantitative analysis of disease progression by body-weight measurement, the inclined plane test, and cage activity, as described above, we defined three time points of "objective onset," as shown in Figure 4. The SCANET results did not allow us to define a time of objective onset, because we could not establish a stable baseline level using the data from the highly variable measurements we obtained, even for wild-type rats. The righting reflex failure was useful for detecting the time point of end-stage disease, which we defined as the generalized loss of motor activity in affected rats. A total of 20 transgenic rats assessed by body weight and the inclined plane test were analyzed for the day of objective onset, end-stage, and duration of the disease. The cage activity data from the eight transgenic rats were obtained simultaneously. The results are shown in Table IV.

The day the transgenic rats reached their maximum body weight was defined as pre-symptomatic onset (113.6 ± 4.8 days of age, black arrowhead in Fig. 4A, Table IV). This onset was judged retrospectively and always preceded the subjective onset (gray shaded region, Fig. 4A), which was determined by observable functional deficits in the open field, such as paralysis of limbs and symptoms of general muscle weakness. The

TABLE IV. Onset, End-Stage, and Duration in Days of Disease in hSOD1 (G93A) Transgenic Rats

Evaluation methods	Body weight and inclined plane (n = 20)	Cage activity (n = 8)
Objective onset		
Pre-symptomatic onset[a]	113.6 ± 4.8 (103–124)	
Muscle weakness onset[b]	125.2 ± 7.4 (110–144)	
Hypo-activity onset[c]		122.8 ± 9.2 (109–139)[c]
Subjective onset (SO)[d]	126.5 ± 7.1 (113–147)	121.3 ± 9.8 (109–140)
End-stage disease (ED)[e]	137.8 ± 7.1 (128–155)	134.1 ± 8.2 (122–149)
Duration[f]		
ED-a[g]	24.3 ± 6.5	
ED-b[h]	12.6 ± 3.5	
ED-c[i]		11.4 ± 1.3

Values are means ± SD.
[a] Maximum of body weight.
[b] Less than 70 degrees in the inclined plane test.
[c] Less than 75% in the mean movements of 70–90 days in the cage activity.
[d] Observable functional deficits.
[e] Righting reflex failure.
[f] Difference in days between ED and each onset;
[g] between ED and pre-symptomatic onset,
[h] between ED and muscle weakness onset,
[i] between ED and hypo-activity onset.

TABLE V. Comparison of the Onset, End-stage, and Duration in Days of Disease in the Forelimb-type and the Hindlimb-type Rats

	Forelimb type (n = 4)	Hindlimb type (n = 14)	General type* (n = 2)
Pre-symptomatic onset[a]	112.5 ± 6.7	114.6 ± 4.3	(108.5)
Muscle weakness onset[b]	125.8 ± 2.8	126.7 ± 7.3	(113.5)
End-stage disease (ED)[c]	134.0 ± 2.4	140.1 ± 7.1	(129.5)
Duration[d]			
ED-a[e]	21.5 ± 8.5	25.5 ± 6.2	(21)
ED-b[f]	8.3 ± 1.0	13.4 ± 3.0	(16)

Values are mean ± SD.
* Values of general-type rats are listed in parenthesis for reference.
[a] Maximum of body weight.
[b] Less than 70 degrees in the inclined plane test.
[c] Righting reflex failure.
[d] Difference in days between ED and each onset;
[e] between ED and pre-symptomatic onset,
[f] between ED and muscle weakness onset.

pre-symptomatic onset was the most sensitive of all the onset measures described in this study (Table IV).

The first day the transgenic rats scored <70° in the inclined plane test was defined as the muscle weakness onset (black arrowhead, Fig. 4B). We could judge this onset prospectively. Muscle weakness onset (125.2 ± 7.4 days of age, Table IV) was usually recorded before or at almost the same time as the subjective onset (8 days before to 1 day after, gray shaded region, Fig. 4B and 126.5 ± 7.1 days of age, Table IV). The day the transgenic rats scored 35° or less on the inclined plane test coincided with the day of righting reflex failure (black arrow, Fig. 4B).

The first day the transgenic rats scored <75% of their baseline movements in the cage activity test was defined as hypo-activity onset (black arrowhead, Fig. 4C and 122.8 ± 9.2 days of age, Table IV). We could also judge this onset prospectively. Hypo-activity onset was recorded 1 day before to 4 days after the subjective onset (SO, shown as the gray shaded region in Fig. 4C and 121.3 ± 9.8 days of age, Table IV). A 0% movement score for cage activity was seen at almost the same time as righting reflex failure (black arrow, Fig. 4C). Although disease onset and end-stage could be objectively defined with these methods, they had a wide range, of about 1 month, because of the diversity of the phenotypes (Table IV).

Differences in Disease Courses Between the Forelimb- and Hindlimb-Type Rats

Because we noticed variability in disease courses among different clinical types of hSOD1 (G93A) rats, we next assessed disease progression in 20 transgenic rats with forelimb- (n = 4), hindlimb- (n = 14), and general- (n = 2) type, using the probability of objective

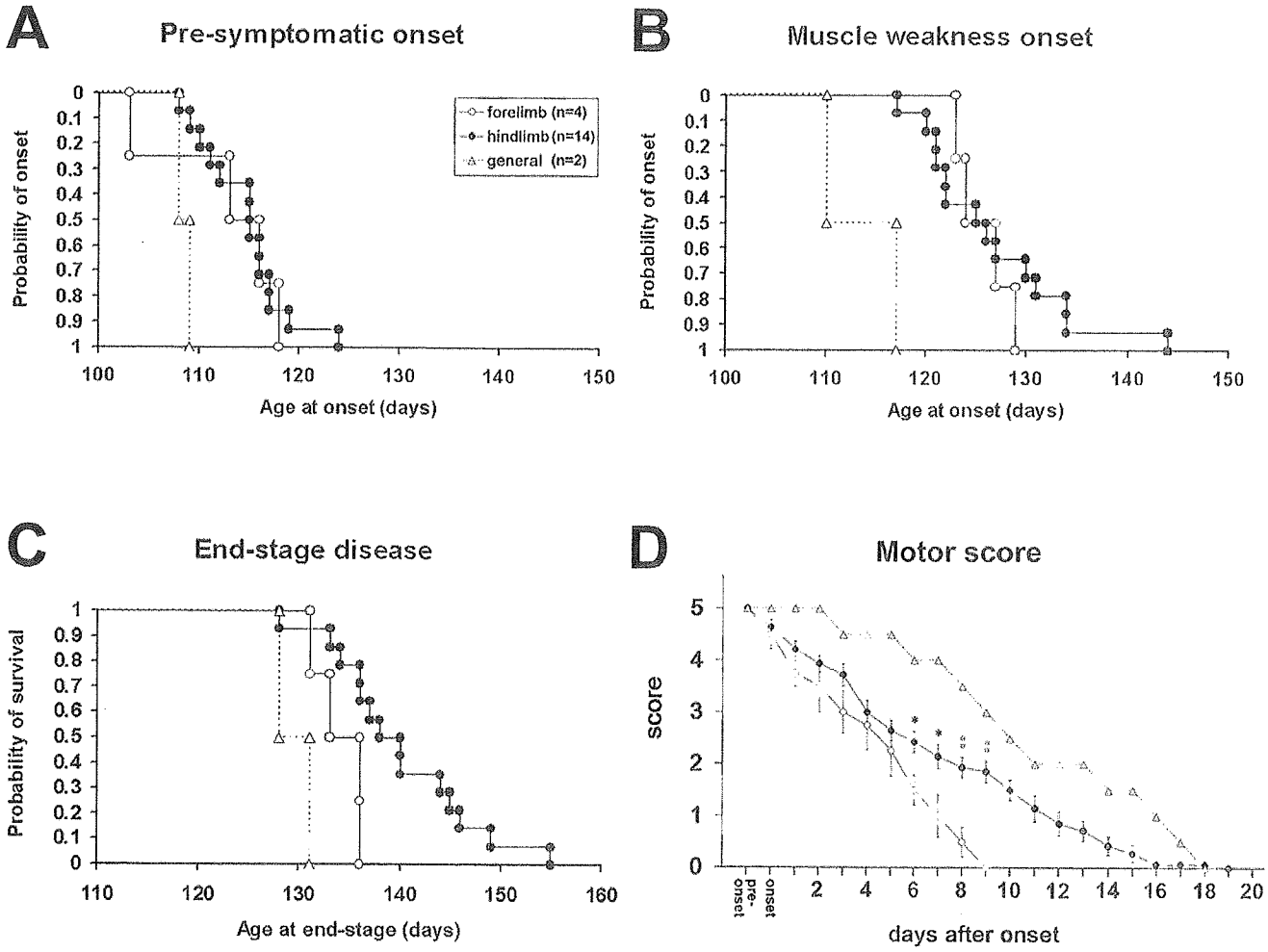

Fig. 5. Comparison of onset, end-stage, and disease progression in the forelimb-type ($n = 4$), and the hindlimb-type ($n = 14$) rats. Data from the general-type rats are also shown as dotted lines. **A,B:** The probability of the objective onsets. We did not see any differences in the probability of the objective onsets defined by body weight measurement (pre-symptomatic onset) and the inclined plane test (muscle weakness onset) between the forelimb- and hindlimb-type rats. **C:** The probability of survival as defined by end-stage disease. Survival was significantly shorter in the forelimb-type than in the hindlimb-type rats ($P < 0.05$, Log-rank test). **D:** Assessment of disease progression using the Motor score. Affected rats were evaluated after muscle weakness onset. The forelimb type worsened more quickly than the hindlimb type. Score decline correlated well with the exacerbation of symptoms in both clinical types, clearly and objectively. Bars = means ± SEM. Statistically significant differences between forelimb and hindlimb types are indicated in the figures. $*P < 0.05$. $**P < 0.01$; two-tailed unpaired Student's t-test.

onsets (pre-symptomatic onset and muscle weakness onset), the probability of survival defined by end-stage disease (failure in righting reflex), and the Motor score (Table V, Fig. 5). We did not see any differences in the objective onsets between the forelimb- and hindlimb-type rats (Fig. 5AB, Table V). However, survival as defined by end-stage disease was significantly shorter in the forelimb-type than in the hindlimb-type rats ($P < 0.05$, Log-rank test, Fig. 5C). Moreover, the duration of the disease calculated from the muscle weakness onset was also significantly shorter in the forelimb-type (8.3 ± 1.0 days) than in the hindlimb-type rats (13.4 ± 3.0 days) (see ED – b, $P < 0.01$, two-tailed unpaired Student's t-test, Table V).

The courses of functional deterioration evaluated by the Motor score after onset (muscle weakness onset) for each clinical type were well represented by the declines in their scores (Fig. 5D). The assessment by the Motor score also showed that disease progression in the forelimb type was more rapid than that in the hindlimb type (Fig. 5D).

Our results raise the question of why this variability in the disease course of each clinical type was observed. We speculated that there might be correlation between clinical type in G93A rats and the amount of locally expressed mutant hSOD1 (G93A) gene product. Therefore, we next investigated expression of the mutant hSOD1 gene in each segment of the spinal cord (cervical, thoracic, and lumbar) in the forelimb- and

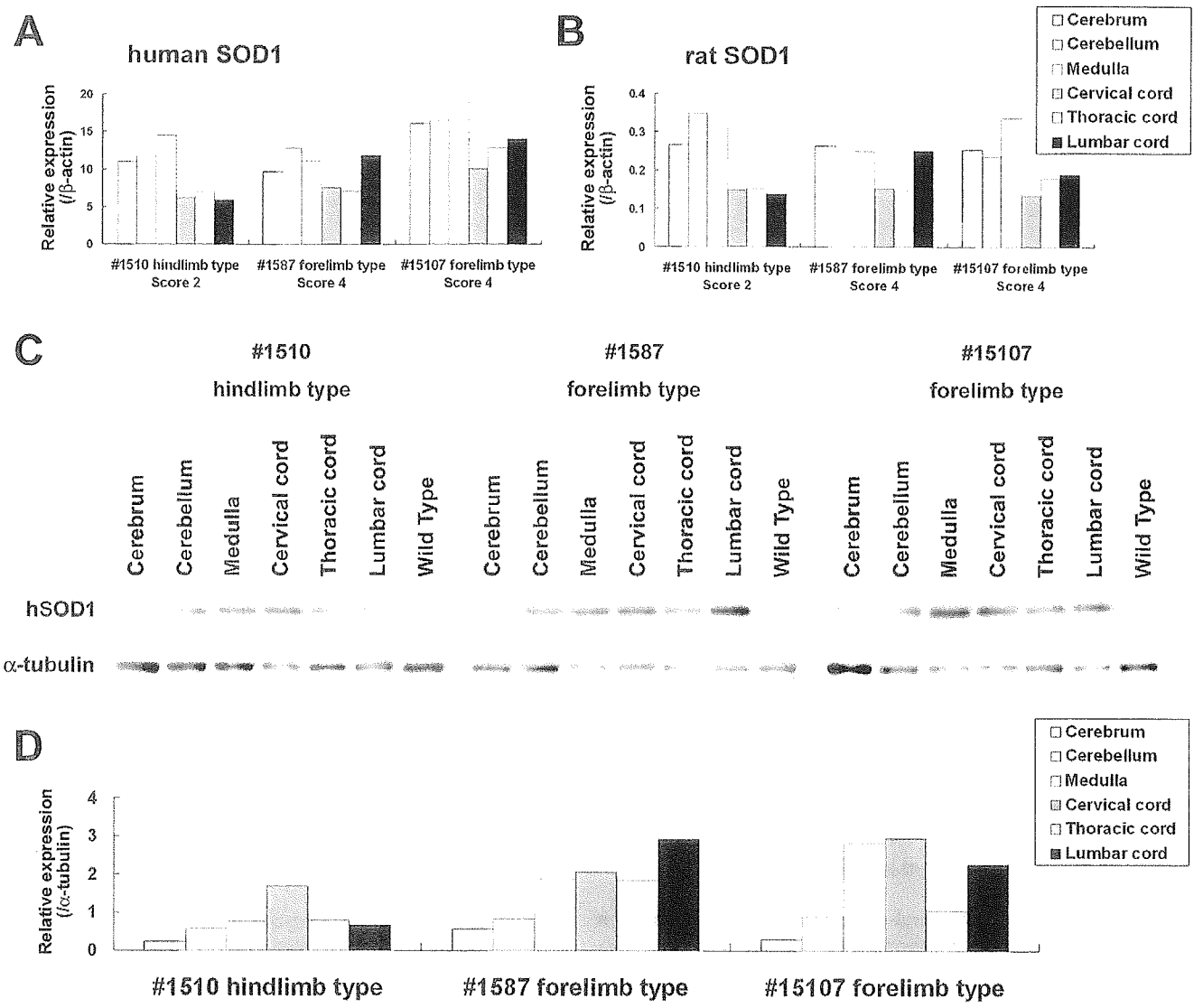

Fig. 6. The expression of mutant hSOD1 mRNA and protein in the cerebral cortex, cerebellum, medulla, and spinal cord (cervical, thoracic, and lumbar) of forelimb- and hindlimb-type rats. **A,B:** The amounts of human (A) and endogenous rat (B) SOD1 mRNA normalized to those of *β-actin* were quantified by real time RT-PCR analysis. **C,D:** Western blot analysis of the mutant hSOD1 protein was carried out in the same rats. Quantitative analysis was carried out with a Scion Image. The amounts of proteins were normalized to those of α-tubulin (D).

hindlimb-type rats by real time RT-PCR and Western blot analysis. However, at least at the stages after the apparent onset of muscle weakness, neither forelimb-type (#1587, Score 4 and #15107, Score 4) nor hindlimb-type rats (#1510, Score 2) necessarily expressed larger amounts of the mutant hSOD1 (G93A) transgene in the cervical cord or in the lumbar cord, respectively, at the mRNA and the protein level (Fig. 6). We also investigated the expression of endogenous rat SOD1 mRNA in the same rats by REAL TIME RT-PCR (Fig. 6B). Distribution of endogenous rat SOD1 mRNA expressed in each segment of the spinal cord showed almost the same pattern as that of mutant hSOD1 mRNA. The expression of endogenous rat SOD1 mRNA was lower than that of mutant hSOD1 mRNA. Thus, we could not detect any definite correlation between the hSOD1 (G93A) transgene local expression profile in the spinal cord and the phenotypes of G93A rats for either the forelimb-type or the hindlimb-type rats (Fig. 6).

Reduction in the Number of Spinal Cord Motor Neurons at Different Disease Stages

We examined histo-pathological changes in the spinal cords of the transgenic rats in comparison with those

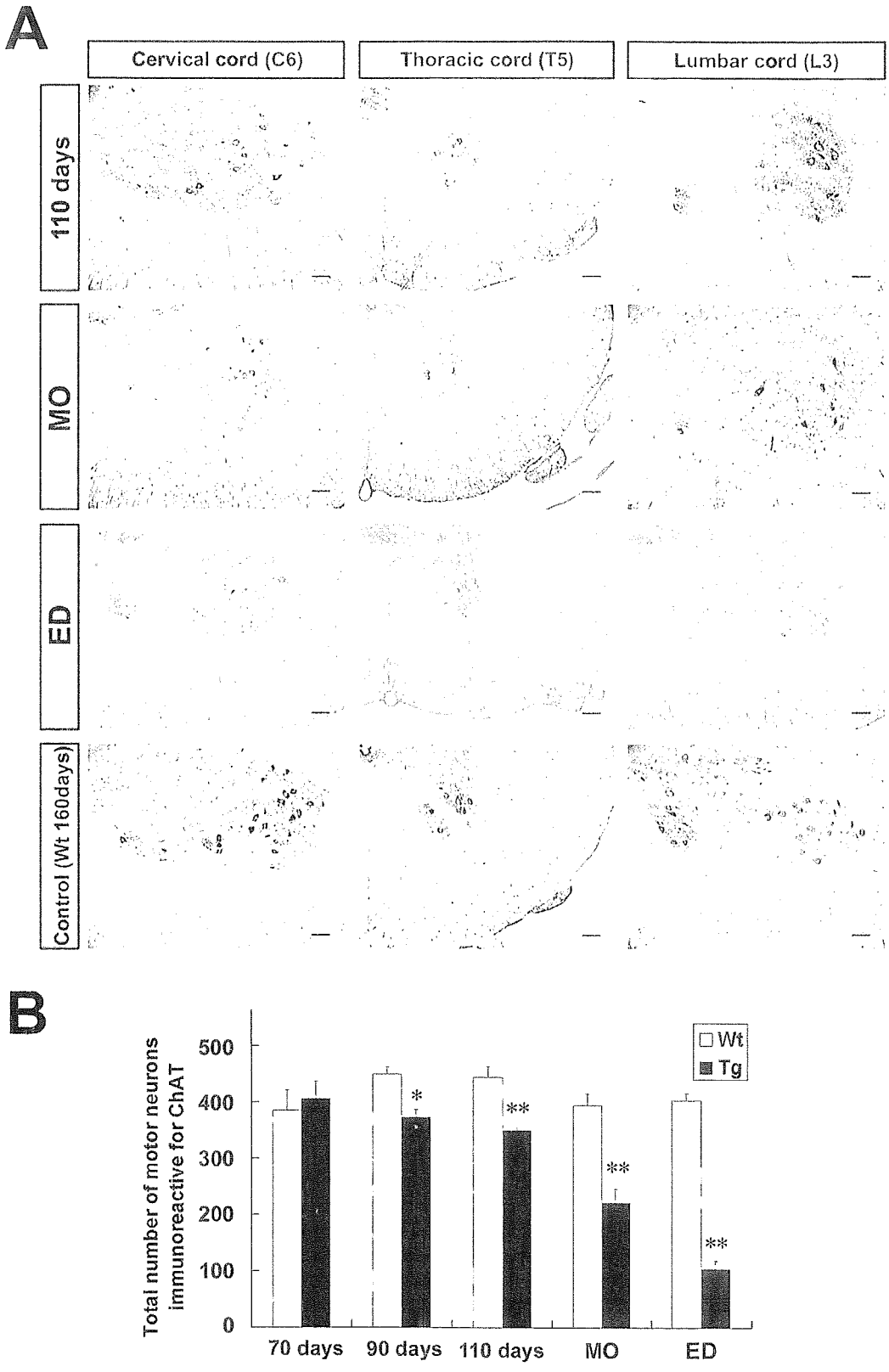

Fig. 7. The loss of motor neurons in the spinal cord of hSOD1 (G93A) transgenic rats at different stages. **A:** Immunohistochemical analysis of the spinal cord of transgenic rats. Transverse sections of the cervical (C6), thoracic (T5), and lumbar (L3) spinal cord of the transgenic rats and their wild-type littermates were stained with an anti-ChAT antibody to label viable motor neurons at the indicated stages (Scale bars = 100 μm). **B:** The number of ChAT immunoreactive motor neurons was counted and is shown in the histograms as the total number of motor neurons in the C6, T5, and L3 segments. This number began to decrease in the transgenic rats at 90 days of age, rapidly declined after 110 days of age, and fell to about 50% and 25% of wild-type rats at the muscle weakness onset (MO, around 125 days) and at end-stage disease (ED, around 140 days), respectively. Bars = means ± SEM ($n = 3$ for each genotype). $^{*}P < 0.05$. $^{**}P < 0.01$; two-tailed unpaired Student's t-test.

of their wild-type littermates at 70, 90, and 110 days of age, when the transgenic rats scored <70° in the inclined plane test (muscle weakness onset), and failed the righting reflex. To quantify the number of spinal motor neurons, we stained spinal cord sections of both groups with an anti-ChAT antibody.

As shown in Figure 7A, the numbers of ChAT immunoreactive motor neurons in the cervical (C6), thoracic (T5), and lumbar (L3) segments of the spinal cord decreased with disease progression. Quantitative analysis of the residual motor neurons showed that the total number of motor neurons in the transgenic rats began to decrease at 90 days of age, rapidly declined after 110 days of age, and fell to about 50% and 25% of the numbers in age-matched wild-type littermates at the time the score was <70° in the inclined plane test (muscle weakness onset) and of righting reflex failure, respectively (Fig. 7B).

TABLE VI. Adequacy of Evaluation Methods in Regard to Practical Use*

	Body weight	Inclined plane	Cage activity	SCANET	Motor score
Objectivity	A	B	A	A	B
Sensitivity	A	B	C	(A)	-
Specificity	C	B	C	C	A
Motivation independence	A	B	B	D	B
Skill requirements	A	B	A	A	B
Cost of apparatus	B	B	D	D	A

*A, more appropriate; B, appropriate; C, less appropriate; D, inappropriate.

DISCUSSION

Factors Underlying the Variability in Phenotypes of hSOD1 (G93A) Transgenic Rats

In previous studies of this G93A rat, only the hindlimb-type has been described, and the variety of phenotypes and variable clinical courses have not yet been mentioned (Nagai et al., 2001). Recently, however, another line of G93A rats backcrossed onto a Wistar background ($SOD1^{G93A/HWr}$ rats) was reported to present two phenotypes, including forelimb-type, and a large inter-litter variability in disease onset (Storkebaum et al., 2005). In the same way, commonly used FALS model mice harboring hSOD1 (G93A) gene have been reported to have clinical variability to some extent, and some of them dominantly show forelimb paralysis (Gurney et al., 1994). In this study, we recognized various clinical types, including forelimb-, hindlimb-, and general-type and established quantitative methods to evaluate disease progression that can be applied to any of the clinical types of this ALS model. We have also shown the variability in disease progression to depend on clinical types, that is, disease progression after the onset was faster in forelimb-type than in hindlimb-type rats. This difference may be due to the aggressiveness of the disease per se because we evaluated the time point of "death" (end-stage disease) according to righting reflex failure (Howland et al., 2002) to exclude the influence of feeding problems (bulbar region) and respiratory failure (level C2–C4).

These findings give rise to the next question; why is this variety of phenotypes and variability in the clinical course observed in the same transgenic line? There are at least three possible explanations. One is that the variation is due to the heterogeneous genetic background of the Sprague-Dawley (SD) rat (i.e., the strain used to generate this transgenic line), which might have led to different phenotypes. This idea is supported by the fact that the SD strain shows a large inter-individual disease variability in other models of neurodegenerative disorders, such as Huntington's disease (Ouary et al., 2000). Similar phenotypic variability takes place in human FALS carrying the same mutations in hSOD1 gene (Abe et al., 1996; Watanabe et al., 1997; Kato et al., 2001), which could be explained by heterogeneous genetic backgrounds. Thus, the present transgenic ALS model rats may be highly useful to understand the mechanisms of bulbar onset, arm onset, or leg onset that are seen in human disease. There may be modifier genes of these phenotypes, which should be identified in the future study.

The second is that there is variability in the expression of the mutant hSOD1 protein. The transcriptional regulation of this exogenous gene could be affected by one or more unknown factors, such as epigenetic regulation, and may not be expressed uniformly throughout the spinal cord of each animal. Therefore, some rats might express mutant proteins more in the cervical spinal cord and others might express more in the lumber cord, possibly resulting in the forelimb type and hindlimb type, respectively. However, we found no definite correlation between local expression levels of the mutant hSOD1 mRNA/protein in the spinal cord and the phenotypes of these animals, using real time RT-PCR and western blot analysis after the onset of muscle weakness, when the clinical type of the transgenic rats could be defined (Fig. 6). Moreover, the pathological analysis showed no correlation between the number of residual motor neurons in each segment and the phenotypes of end-stage animals. However, because >50% of spinal motor neurons have already degenerated at the stage of muscle weakness onset, whether local expression of the mutant hSOD1 gene and segmental loss of motor neurons correlate with the clinical types of G93A rats should be further investigated by analyzing younger animals at a stage when motor neuron loss has not progressed as much.

The third explanation involves a structural property of the mutant hSOD1 (G93A) protein itself. It is now thought that mutations in the hSOD1 gene may alter the 3-D conformation of the enzyme and, in turn, result in the SOD1 protein acquiring toxic properties that cause ALS (Deng et al., 1993; Hand and Rouleau 2002). For instance, the hSOD1 (G93A) mutant protein has been reported to be susceptible to nonnative protein–protein interactions because of its mutation site and unfolded structure (Shipp et al., 2003; Furukawa and

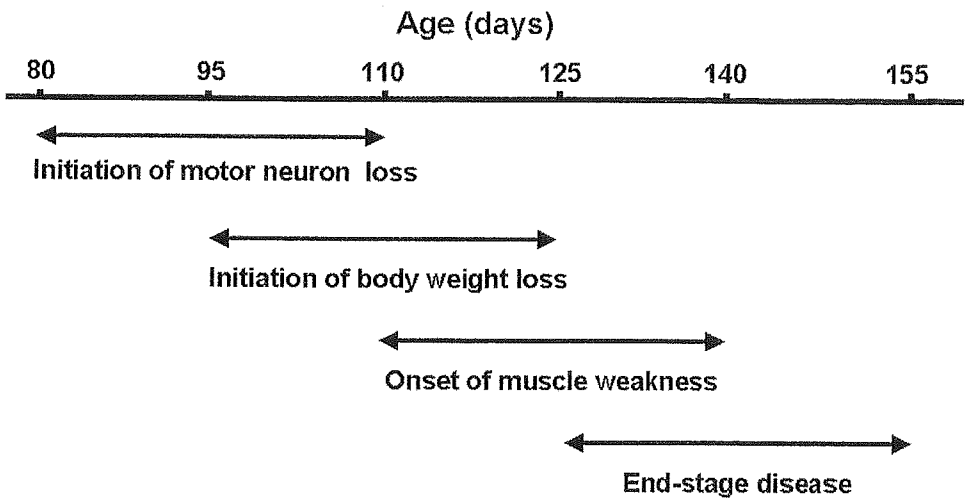

Fig. 8. Four stages of disease progression in hSOD1 (G93A) transgenic rats. The disease progression can be classified into four stages as shown. The range for each stage is about 1 month and overlaps approximately 2 weeks with the next stage.

O'Halloran, 2005), suggesting that the G93A mutation might accelerate the formation of SOD1 protein aggregates, which may ultimately sequester heat-shock proteins and molecular chaperones, disturb axonal transport or protein degradation machineries, including the ubiquitin-proteasome system (Borchelt et al., 1998; Bruening et al., 1999; Williamson and Cleveland 1999; Okado-Matsumoto and Fridovich 2002; Urushitani et al., 2002). Curiously, the mutated hSOD1 (G93A) protein is more susceptible to degradation by the ubiquitin-proteasome system and has a shorter half-life than other mutants (Fujiwara et al., 2005), suggesting that it may cause more unstable toxic aggregates in the spinal cord than other mutations. The degradation rate is also affected by environmental factors unique to each animal, such as the progressive decline of proteasome function with age (Keller et al., 2000), and these factors could contribute to the variability of the clinical course of G93A rats.

Taking all these findings into consideration, the mutated hSOD1 (G93A) protein may gain properties that are responsible for a variety of phenotypes and variability in the clinical course of the affected animals.

Characteristics of Different Methods for Assessing hSOD1 (G93A) Transgenic Rats

The ideal measure is not influenced by the judgment of the observer, sensitive to small abnormalities, specific to detect pathologic events that are related to pathogenesis of the ALS-like disease, not influenced by the motivational factors of rats, minimal in the requirements for skill in the observer, and inexpensive to carry out. We assessed each evaluation method by the categories in regard to practical use as shown in the Table 6.

The initiation of body weight loss seems to be an excellent marker to detect the onset and should be highly recommended. Muscle volume might have already started to decrease, even in the period of continuous weight gain, as reported for hSOD1 (G93A) transgenic mice (Brooks et al., 2004). As a result, it could detect an abnormality relatively earlier than subjective onset. The inclined plane test is considered to be the least defective method of all. It could objectively and specifically detect the decline in the muscle strength of these ALS model rats as a muscle weakness onset almost at the same time of the subjective onset. The cage activity measurement and SCANET require very expensive apparatus, and are limited by the availability of funds and space for making the measurements. Although SCANET test was most sensitive among these measures, it seems inappropriate for the statistical analysis, and does not add any more information than that obtained through simple observation of the rats because the performances of the rats might be severely affected by the extent of their motivation to explore. Motor score can specifically assess disease progression of each clinical type and is valuable in keeping the experimental costs at a minimum.

Correlation Between the Loss of Spinal Motor Neurons and Disease Stages

This study clearly shows the variable clinical course of G93A rats. According to our behavioral and histological analyses, we can divide the disease course of this transgenic model into four stages, whose durations have a range of about 1 month, as shown in Figure 8. Furthermore, we have established the pathological validity of the performance deficits detected by each measure of disease progression. "Initiation of motor neuron loss" was defined as a statistically significant decrease in the number of spinal motor neurons, which was found at around 90 days of age, but not 70 days of age (Fig. 7B). This coincides with, and seems to be sensitively detected by the marked difference in SCANET scores that begins at around 90 days of age (Fig. 3D–F). The "initiation of body weight loss" was usually detected at around 110 days of age as the peak body weight (pre-symptomatic onset, 113.6 ± 4.8 days of age, range = 103–124, Table IV). This stage coincides with the initiation of a rapid decline in the number of motor neurons at around 110 days of age (Fig. 7B). "Onset of muscle weakness" was detected at around 125 days of age, as assessed by the